Preparing samples from whole cells using focused-ion-beam milling for cryo-electron tomography

Felix Roman Wagner[1,4], Reika Watanabe[1], Ruud Schampers[2], Digvijay Singh[1], Hans Persoon[2], Miroslava Schaffer[3], Peter Fruhstorfer[2], Jürgen Plitzko[3], Elizabeth Villa[1]

[1]Department of Molecular Biology, Division of Biological Sciences, University of California San Diego, 9500 Gilman Dr. La Jolla, CA 92093, USA.
[2]Thermo Fisher Scientific, Achtseweg Noord 5, 5651 GG Eindhoven, Netherlands.
[3]Department of Molecular Structural Biology, Max Planck Institute of Biochemistry, Am Klopferspitz 18, 82152 Martinsried, Germany.
[4]Present address: Department of Molecular Biology, Max-Planck-Institute for Biophysical Chemistry, Am Faßberg 11, 37077 Göttingen, Germany.

*Email: evilla@ucsd.edu. Twitter: @TheVillaLab. Website: villalab.ucsd.edu

KEYWORDS Cryo-focused-ion-beam milling, Cryo-electron tomography, Dual beam microscope, Lamellae, *In situ* protein structural analysis, Structural cell biology, FIB milling, cryo-FIB milling, cryo-ET, cryo-EM, cryo-FIB, CLEM, correlated light, electron microscopy, cryo-CLEM, fluorescence microscopy

EDITORIAL SUMMARY: High-resolution structural analysis of macromolecular complexes in native and unperturbed conditions by cryo-electron tomography requires extremely thin samples. This protocol describes how to prepare thin specimens using focused-ion-beam (FIB) milling from frozen cells on grids.

TWEET A detailed Protocol for #FIBmilling of frozen cells on grids for #cryoET analysis #cryoEM @TheVillaLab @ReikaWatanabe2 @dgvjayS
COVER TEASER cryo-FIB-milling for native protein structure analysis

Up to four primary research articles where the protocol has been used and/or developed:

1. Mahamid, J. *et al.* Visualizing the molecular sociology at the HeLa cell nuclear periphery. *Science (80-.).* 351, 969–972 (2016).

2. Chaikeeratisak, V. *et al*. Viral Capsid Trafficking along Treadmilling Tubulin Filaments in Bacteria. Cell 177, 1771-1780.e12 (2019).

3. Khanna, K. *et al*. The molecular architecture of engulfment during Bacillus subtilis sporulation. Elife 8, (2019).

4. Watanabe, R. *et al*. The *in situ* structure of Parkinson's disease-linked LRRK2. bioRxiv (2019).

Abstract

Recent advances have made cryo-electron microscopy a key technique for achieving near-atomic resolution structures of biochemically isolated macromolecular complexes. Cryo-electron tomography (cryo-ET) can throw an unprecedented insight into these complexes in the context of their natural environment. However, the application of cryo-ET is limited to samples that are thinner than most cells, thereby considerably reducing its applicability. Cryo-focused-ion-beam milling (cryo-FIB milling) has been used to carve (micromachining) out 100 to 250 nm thin regions (called lamella) in the intact frozen cells. This procedure opens a window into the cells for high-resolution cryo-ET for the structure determination of biomolecules in their native environment. Further combination with fluorescence microscopy allows users to target cells or regions of interest for the fabrication of lamellae and cryo-ET imaging. Here, we describe how to prepare lamellae using a microscope equipped with both FIB and scanning electron microscopy (SEM) modalities. Such a microscope (Aquilos Cryo-FIB or Scios equipped with cryo-stage) is routinely referred to as a dual beam microscope (DualBeam™), and they are equipped with a cryo-stage for all operations in cryogenic conditions. The basic principle of described methodologies is also applicable for other types of dual beam equipped with a cryo-stage. We also briefly describe how to integrate fluorescence microscopy data for target milling and critical considerations for cryo-ET data acquisition of the lamellae. Users familiar with cryo-electron microscopy who get basic training in dual beam microscopy can complete the protocol within 2-3 days allowing for several pause points during the procedure.

Introduction

Transmission electron microscopy of cryo-preserved biological specimens (cryo-EM) provides information about the intact structures of macromolecules without any artifacts stemming from fixation, dehydration, or staining. In the single-particle analysis mode, three-dimensional structures of macromolecular complexes are obtained by taking thousands to millions of images of identical molecules that have been biochemically isolated[1–3]. However, high-resolution structures of isolated proteins might not represent their functional conformation or complexity that is dependent on their native cellular environment and the presence of interaction partners. Furthermore, in some cases, the structural preservation of the complexes is compromised when extracted from their natural environment, rendering isolation intractable.

Cryo-electron tomography (cryo-ET) can be used to image these structures in their natural environment in 3-D[4]. However, cryo-ET is limited by the thickness of the sample. When aiming for protein structural analysis, the sample should be of a similar thickness to the mean free path of the electrons used (typically 300 keV) traveling through the material under study; for biological samples, ~ 280 nm[5]. As a result, samples thicker than 500 nm yield little contrast and require high electron doses that significantly limit the resolution or prevent acquisition altogether. This limitation has confined the applicability of cryo-ET to naturally thin regions such as small prokaryotic cells[6–10], protrusions or peripheral regions of eukaryotic cells[11–14], and to isolated organelles or biochemically reconstituted systems[15–22]. An established alternative is the use of a microtome to cut thin sections of cells that have been high-pressure frozen[3,23,24]. While the ease of use of this technique has improved recently[25], non-homogenous distortions to the sample occur during cutting resulting in artifacts.

These artifacts can not be easily corrected for when aiming for high-resolution structural determination using subtomogram averaging[22,26,27] or performing quantitative analysis that requires combining data sets.

Focused-ion-beam (FIB) milling has been adapted to cryogenic temperatures and is being increasingly applied to cellular samples as a new artifact-free preparation method. It makes use of a beam of focused gallium ions that pass over the sample sputtering away atoms, thus carving out thin regions of cellular material that comply with the requirements of cryo-ET. Different implementations of cryo-FIB milling (also simply referred to as milling) for biological samples have been realized[28–37], allowing the application of cryo-FIB milling to cells that can be deposited on grids. Recent results suggest that its applicability to tissues is within reach[30,33,36,38–40]. Although the tools and software have considerably improved over the recent years, the yield remains low due to cumbersome steps in the protocols which require an experienced user.

Here we detail the steps needed to generate lamellae samples using cryo-FIB milling of frozen cells on EM grids using a dual beam microscope equipped with a cryo-stage for subsequent cryo-ET [31,41–46]. When protein or organelles of interests are fluorescently labeled, targeted milling of regions of interest in cells can be performed by prior imaging of grids with fluorescence microscopy[47,48]. We also outline the deviations from routine cryo-ET required during data acquisition on these samples. The protocol specifically details the preparation of lamellae for mammalian cells, but the workflow is easily adaptable to other cell types. The procedures described in this protocol are optimized for the commercially available Aquilos Cryo-FIB and the previous version of the dual beam microscope Scios repurposed with the cryo-stage from Thermo Fisher Scientific (TFS). However, the basic principle of described methodologies is also applicable for other types of dual beam microscopes equipped with a cryo-stage.

The overview of the procedure

Figure 1 presents the cellular cryo-electron tomography workflow described in this protocol. The cells are either grown directly on EM grids or are deposited on the grid (Steps 1-13) right before plunge freezing. The plunge freezing of EM grids is done in a commercial or homemade plunger (Steps 14-15). During this protocol, the grids undergo several manipulations and transfer events. In order to ensure the mechanical stability of the grids, the plunge-frozen EM grids are mounted into the solid metal ring, called Cryo-FIB AutoGrid (TFS) (Steps 16-23). When regions or proteins of interest for cryo-ET are fluorescently labeled, fluorescence microscopy can be performed after freezing to identify cells or regions of interest for targeted milling. Such microscopy would require the light microscope equipped with the cryo-cooled stage (Cryo-fluorescence microscopy; Step 24). In cases where cells firmly adhere to EM grids, fluorescence microscopy analysis of cells on EM grids before freezing using a conventional fluorescence microscope can also be done to identify cells of interest. The EM grids are loaded into the cryo-SEM/FIB dual beam microscope for milling to create lamellae, which is the major part of the procedure (Steps 25-101). Subsequently, the lamellae are imaged by cryo-TEM (Steps 102-106) followed by tomogram reconstruction (Step 107) and qualitative and quantitative image analyses, including organelle segmentation, protein structural determination using subtomogram averaging (not covered here).

Level of expertise needed to implement the protocol

The protocol described represents an additional procedure in sample preparation before cryo-ET. Thus, we assume that the scientists implementing the protocol are already familiar with cryo-ET techniques and the intricacies of preparing and handling cryo-samples. In addition, scientists following the protocol should become familiar with a dual beam microscope: routine training for room temperature use of the equipment suffices. The user should also be familiar with various manipulations of cells in culture.

Applications of the method

The protocol describes sample preparation for cryo-ET using cryo-FIB milling of cells that have been grown or deposited on EM grids. The protocol has been successfully used to reveal the native structure of large macromolecular assemblies within cells, that are impossible to be extracted from cells without compromising their structural integrity. Examples of such reveals include nuclear pore complex[44], bacterial cytoskeleton[42], nucleus-like structure[45], various stages of viral particles within infected bacterial cells[42], bacterial cell wall structure[41,46], and Parkinson causing pathogenic proteins bound to cellular microtubules[49]. Such structural analysis has allowed quantitative assessment of how these structures are arranged within their native environments. Modifications of the protocol described here are under development to expand its applicability to large cells and tissue and also increase the ease/throughput of sample preparation by automation[30,33,36,38,39,50–52]. Micro Electron Diffraction (MicroED), a new method that collects electron diffraction patterns from small protein crystals using cryo-EM, has rapidly emerged as a methodology for protein structure determination[53]. This technology has proven valuable to determine structures where crystals cannot be grown to a size amenable to X-ray crystallography. However, many crystals are still too big for cryo-EM, and cryo-FIB milling is being used to gently micro-machine crystals, without affecting its crystalline arrangement, to a size amenable for MicroED[37]. The FIB-milling has also been widely used to study other heat or oxygen-sensitive soft materials, such as solar cells, semiconductor devices, and batteries[54].

Alternative methods

This protocol was developed to visualize macromolecular complexes inside cells in a near-native environment. An alternative established method is the use of a cryo-microtome to cut thin sections of cells and tissue[55–63]. This methodology has become easier to use, is more cost-effective than cryo-FIB milling. However, cryo-microtome presents compression artifacts that prevent high-resolution structural and quantitative analyses. When a high level of detail is not necessary, other cryogenic techniques to study the ultrastructure of cells can be used, such as soft X-ray cryo-tomography[50,64,65], which has been successfully combined with cryo-light microscopy[66,67], and cryo-STEM tomography[68,69] that can be combined with chemical imaging. These techniques have the advantage of being able to image thicker samples (thus circumventing the need for thinning for many samples) and can thus cover larger cellular volumes, albeit at lower resolution. When even larger volumes are needed, the FIB-milling (to ablate the top surface) followed by SEM-imaging of the exposed top surface (FIB-SEM imaging) is performed sequentially to create Z-stacks of SEM image of the entire large volume. Although FIB-SEM imaging provides limited contrast and resolution[70]. Finally, when the fine details of structural preservation are not relevant to the question under study, embedded samples can be used in the above modalities: serial section electron tomography[71] and FIB/SEM of tissue[72,73]. Another exciting methodology is the incorporation of a microtome inside an SEM chamber[74,75]. The embedded samples have the critical advantage of sustaining radiation damage better than cryo-samples, which, together with the stain, provide better imaging contrast. The embedded samples also provide the ability to image large cellular and even tissue volumes and the ability of molecular tagging, which is an exciting and active area of development[76–80].

Advantages and Limitations

The advantage of this protocol lies in its ability to go beyond an ultrastructural description into a *bona fide* structural and quantitative study of macromolecules within cells. This advantage is enabled by structural preservation of the cellular structures through vitrification, and high-resolution information afforded by thinning of the samples. These advantages are especially relevant when studying the structural features of macromolecules that would be altered or "hidden" by other sample preparation techniques. For instance, high-resolution structure determination is not only unfeasible when samples are negatively stained, but a direct interpretation of the structure is not straightforward due to the stain. Other methods described above use cryogenic samples, which are structurally preserved but lack the resolution to identify molecular complexes or to do quantitative analysis.

The protocol has limitations that should be considered before its application. The size of the cells under study must be of a size that vitrification can be achieved with plunge freezing (maximum ~10 μm thickness). Many mammalian cells are beyond this limit, and in this case, the high-pressure freezing method followed by cryo-sectioning or FIB lift-out methods needs to be used as mentioned above. Unlike conventional serial sectioning TEM microscopy[71] or FIB/SEM volume imaging[72,73], this protocol does not allow us to image outside of lamellae once lamella is formed, therefore any biological information present outside of lamella has to be obtained before milling.

In summary, the choice of the technique must be made according to the biological questions. To our knowledge, no other method can deliver the resolution and preservation of this protocol when studying macromolecular structures in their intact natural environment inside cells grown or deposited on EM grids. On the other side, this level of detail might not be required to answer the biological question under study. Thus, by providing a detailed protocol here, we hope that readers are able to choose a suitable methodology for their specific biological questions.

Experimental Design

Sample preparation. Cells for focused-ion-beam milling can be frozen by optimizing a standard protocol for either a homemade or a commercial plunge freezer. Adherent mammalian cells can be grown directly on EM grids coated with extracellular matrix allowing their attachment (described in Steps 2-11 of the Procedure). Since conventional copper EM grids are cytotoxic, we use gold EM grids. We aim to have one isolated cell grown in each EM grid mesh for better freezing. Bacteria, yeast cells, and suspension cells can be added on glow-discharged copper EM grids before plunging (Step 12). For bacterial samples, a continuous single layer of cells over the whole EM grid ensures a high hit rate during milling while also allowing the sample to freeze fast enough to form vitreous ice. Yeast cells should form small clusters. Therefore, the cluster size and density have to be limited for ideal vitrification throughout the cluster. One needs to optimize the bacteria or yeast cell concentration (in ~ 5 μL volume) to be added to the EM grid before plunging to meet the conditions mentioned above.

Grids preparation: Choice of grids, plunging procedure, and mounting onto AutoGrids. We use EM grids with a perforated carbon support foil, e.g., Quantifoil grids (Quantifoil Micro Tools, Jena, Germany). The cells are either grown directly on EM grids or are deposited on the grid right before freezing after being grown in liquid medium (Figure 1a). The former often requires the use of gold grids to avoid cytotoxicity effects from copper or other materials. The grids are blotted to wick away excess liquid and immediately plunge frozen in a liquid cryogen such as liquid ethane

or propane/ethane 50/50 mixture, cooled down by liquid nitrogen. The rapid cooling traps water in an amorphous state, preventing the formation of ice crystals, which are damaging to the structural integrity of macromolecules[81]. Thus, the vitreous character of the sample results in a fixed specimen preserved in a near-native state. The plunge freezing, or vitrification step, is done in a commercial or homemade plunger. Once frozen, the grids have to be kept as low as possible close to cryogenic temperature (less than -150 °C). Utmost care must be taken to minimize sample contamination with humidity/ice particles during storage, transfer, and microscope observation. This contamination-free cryogenic condition is maintained by keeping the grids either in liquid nitrogen or under high vacuum and active cooling. During this protocol, the grids undergo several manipulations and transfer events. In order to ensure the mechanical stability of the grids and lamellae and to load at the Titan Krios TEM microscope, we routinely mount the EM grids into metal rings called FIB-AutoGrids from TFS after plunge freezing before cryo-FIB milling (**Fig. 2**). The FIB-AutoGrid has a milling slot that allows for sample milling at lower ion beam incident angles and also increases the area on the grid accessible by the focused ion beam at a given low tilt angle (**Fig. 2**). Alternatively, standard AutoGrids from TFS can be utilized but would require milling at higher angles (**Fig. 2-3**).

FIB milling instruments. This protocol describes the steps required to prepare samples using cryo-FIB milling suitable for cryo-ET with commercially available Thermo Fisher Scios and Aquilos systems equipped with a cryo-stage. Laboratories that do not have this equipment at hand can adapt existing dual beam microscopes with commercially available cryo stages to implement this workflow[28,32–35,82].

Thermo Fisher Scios and Aquilos systems combine a scanning electron microscope (SEM) and a focused ion beam (FIB). These two beams are located at 52° from each other so that a head-on view in one beam results in a tilted view on the other (**Fig. 3a-b**). The FIB system works similarly to an SEM but uses a focused beam of gallium ions instead of electrons. Depending on the energy of the gallium ions, the intensity of the beam, and scanning time, the FIB can be used to image the sample or to sputter atoms from it, micromachining it into different shapes. During the milling process, the SEM is used for navigation and assessment of the sample. In order to generate the lamellae, the FIB has to be incident on the sample at grazing angles, i.e., minimal angles to the plane of the grid (**Fig. 3c-d**). The stage is cryo-cooled by the continuous flow of cryo-cooled nitrogen around it (**Fig. 4a-b**). The cryo-stage of the Aquilos is motorized and preserves all its degrees of freedom, namely translation (X, Y, Z), in-plane rotation 360° (R), and tilt up to 45°(T) at the cryogenic temperature (**Fig. 4c-d**).

Preparation prior cryo-FIB milling: Sample loading, correlation with fluorescence imaging, and Platinum layer deposition. When the correlation with fluorescence image is possible for targeted milling and subsequent cryo-ET, the grids have to be imaged by fluorescence microscopes before milling (**Fig. 1a**). The EM grids mounted in AutoGrids are loaded into the dual beam by mounting them onto a shuttle that is transferred into the microscope under vacuum conditions. The shuttle can hold two AutoGrids at an angle, so that after loading the grids are placed 45° to the electron beam, which corresponds to an angle of - 7° to the FIB, i.e., the back of the grid (**Fig. 3c**). Tilting the stage by ~ 14 – 25° thus results in effective milling angles of ~ 7 – 18°, presenting the grids at grazing angles suitable for milling lamellae (**Fig. 3d**)

The AutoGrids loading into the transfer shuttle is performed using the sample preparation station (preparation station) (**Fig. 5**). The shuttle is grabbed by a specially designed cryo loader

device transfer rod (**Fig. 6**), that can be attached to the preparation station and be vacuum pumped (**Fig. 5d**). On the microscope, the transfer rod is attached to the quick loader system in order to insert the shuttle into the microscope under vacuum (**Fig. 4a and Fig. 6b**).

After sample loading into the dual beam microscope, overview SEM images of grids are taken, and correlation with fluorescence image could be performed to identify the cells or areas to be milled (**Fig. 1a**). The grids surface within a ~ 600 µm radius around the grid's midpoint is to be selected for lamellae production (~ 5 meshes on a 200-mesh EM grid) for subsequent high-resolution cryo-ET with TFS Titan Krios (**Fig. 2b**). Lamellae further away from the center of the EM grid might be inaccessible to the stage in the TEM. Within these areas, cells that satisfied the following conditions are targeted for milling: (1) isolated cell. Clustered mammalian cells frequently result in non-vitreous ice inside of cells. (2) located within the center of the grid square mesh covered with the intact carbon film. The adjacent grid bar limits the tilt angle during cryo-ET. The lamellae produced on cracked carbon films are prone to be lost during sample transfer to TEM.

It is highly recommended to cover the sample with a thick organometallic platinum layer (several hundred nanometers to a few micrometers) by Gas injection system (Pt GIS deposition) (**Fig. 7a**) before milling to reduce charging of samples during imaging and milling, give extra support of lamellae during sample transfer, and to minimize the formation of so-called curtains caused during milling. Curtains arise from differences in the density of the various biological materials. The continuous platinum layer on the surface diminishes the creation of curtains by presenting a uniform and dense layer of material to the ion beam (**Fig. 7b**).

FIB milling procedure. The precise milling is achieved by setting the milling patterns where FIB passes over the samples to ablate unnecessary materials to leave a thin-sliced region of interest to be imaged by cryo-ET. The typical example of a milling pattern is shown (**Fig. 7c**). Wider lamellae are more prone to bend and break during milling and also to be lost or cracked during sample transfer. The milling angle determines the length of the lamellae and thinner the cell height is, shallower milling angle is required to obtain the same length of lamellae (**Fig. 7b**). The milling of a lamella takes place in a multi-step process (**Fig. 7c**). At first, a 2 – 3 µm lamella is defined by placing milling patterns above and underneath the lamella-to-be, and that material is milled away with a relatively high current. The higher the ion beam current, the faster the milling process, albeit at the cost of more substantial beam-induced damage and less precise milling. Thus, after the first rough milling, the patterns are placed closer together, and the next sample layer above and underneath the lamella-to-be is milled away with a lower current beam. By repeating this step, the beam-induced damage to the lamella is minimized while optimizing the milling time. In the last milling step, the lamella is polished, that is, its surface is smoothened, and its final shape and thickness are defined. The lamella thickness could be roughly estimated by comparing the different degrees of transparency of lamellae in SEM images taken at different voltages (2 kV versus 5 kV)[83]. Recently it has been reported that the creation (via cryo-FIB milling) of two narrow gaps on both sides of the lamella called "micro-expansion joints" drastically reduces bending and breakage of lamella during the cryo-FIB milling process by absorbing tension and material motion on EM grids[84]. This strategy has worked exceedingly well in our milling workflow and is now being routinely implemented.

At the end of lamella production, sputtering very thin platinum metal layer (several angstroms to a few nm) improves the electrical conductivity of the lamellae surface which is particularly useful when the phase-plates are used during TEM imaging[44]

Considerations for subsequent cryo-ET. Since the ion beam approaches the cells at a certain angle from the grid surface, the resulting lamella is pre-tilted in comparison with EM grids (**Fig. 7b**). During cryo-ET, where the sample is tilted, the tilt axis should be perpendicular to the milling direction to ensure the remaining bulk cell materials sustaining the lamellae do not "shadow" the image. This geometry of the tilt-axis also ensures the tracking and focus areas during tomography acquisition are at the same height along the optical axis as the Record area. Considering the limitation of the maximum tilt angles possible at TEM, shallow tilt angles of lamellae allows more evenly distributed imaging during tilting toward both directions, resulting in better TEM data quality.

MATERIALS

Biological Materials

- In this protocol, we demonstrate our procedure using NIH/3T3 mouse (Mus musculus) embryonic fibroblast cells (ATCC, # CRL-1658; RRID:CVCL_0594). We have also successfully used our approach with HEK293 cell, U2OS cells, MDCK cells, and BSC-1 cells. And we anticipate this protocol should be compatible with various other cell lines with similar thickness and size.
  ! CAUTION The cell lines used should be regularly checked to ensure they are authentic and are not infected with mycoplasma.

Reagents

- Milli-Q water
- CO_2 gas for incubator (Praxair, 12-14-19-00)
  ! CAUTION Ensure adequate ventilation to avoid asphyxiation
- Liquid N_2 (Praxair, Airgas. More than 100 psi pressure tank is required for Aquilos N_2 gas supply)
  CRITICAL When the liquid N_2 comes in contact with samples it should free of any water contamination
  ! CAUTION Ensure adequate ventilation to avoid asphyxiation and use personal protective equipment, such as safety glasses, face shield, and cold-resistant gloves
- Dry N_2 gas
  ! CAUTION Ensure adequate ventilation to avoid asphyxiation
- Ethane Grade 2.0 (Praxair part# ET 2.0-G) or a 50% (vol/vol) High Purity Ethane, 50% (vol/vol) High Purity Propane mixture (Airgas or Praxair, special order)
  ! CAUTION Avoid sparks and ensure adequate ventilation
- Trypsin-EDTA (Trypsin 0.25% (wt/vol), EDTA 0.53 mM) (Gemini Bio-Products # 400-151)
- DPBS, no calcium, no magnesium (Dulbecco's phosphate-buffered saline, Life technologies # 14190-144)
- Trypan Blue Solution(Life technologies # 15250-061)
- 1 M HEPES (Life technologies # 15630080)
- DMEM (Dulbecco's Modified Eagle Medium, Life technologies #11995065)
- HyClone Bovine Calf Serum (GE Healthcare # 16777-206)
- HyClone Penicillin-Streptomycin (GE Healthcare # SV30010)
- Fibronectin Bovine Plasma (EMD Millipore # 3416311MG)

Equipment

General Equipment/consumables

- CO_2 incubator (Heracell CO_2 Incubators, Thermo Scientific)
- Biological safety cabinet
- Chemical hood (for the baking chamber)
- Inverted light microscope to check cell confluence and attachment state on the EM grids (Axio Vert.A1, Carl Zeiss Microscopy, LLC)
- Hemocytometer (3200, Hausser Scientific Partnership)
- Cell culture dish with cover, sterilized, 10cm (353003, FALCON)
- Microscope slide, glass (48300-047, VWR), sterilized with 70 % (vol/vol) ethanol and well dried
- Parafilm (152-68319-656, Heathrow Scientific)
- Optional: 35 mm Dish | No. 1.5 Coverslip | 14 mm Glass Diameter | Uncoated (MatTek P35G-1.5-14-C)
- Pipettes and pipette tips
- 15 ml or 50 ml conical tubes (352196, 352098, FALCON)
- Filter paper, e.g., Whatman grade 1 (1001-090, Whatman)
- Surgical masks (AM101, High Five Products Inc)
- Felt-tip pen

Specific Equipment/consumables

- Aquilos Cryo-FIB or any dual beam microscope system equipped with cryo system (FEI, Eindhoven, Netherlands)
- GIS with platinum (Trimethyl [(1,2,3,4,5-ETA.)-1 Methyl-2, 4-Cyclopentadien-1-YL] Platinum) ! CAUTION Please refer to the material safety data sheet of the organometallic compound to ensure its careful handling.
- Preparation base/ Preparation base bottom
- Shuttle for AutoGrids™
- Transfer rod, el al
- Sample bake-out box to safely remove the depositions of the organometallic compound (GIS) and platinum (Platinum sputtering) from the Shuttle for AutoGrids™
- PELCO easiGlow Glow Discharge System (#91000)
- Plunge freezer, homemade or commercial
- Tweezers for EM grid and FIB-AutoGrid handling (PELCO ESD Ergo Tweezers)
- Large tweezers for handling AutoGrid boxes in transport dewars
- EM grids, gold if used for cell culture (Quantifoil R 1/4, 200 mesh, gold, EMS)
- Grid boxes (TED PELLA, Prod# 160-42)
- Grid box opening/closing tool (FEI, Part-No. # 9432 909 97671)
- AutoGrid boxes (FEI, Part-No. # 9432 909 97621)
- AutoGrid Assembly Workstation (FEI, Part-No. # 1000068) or AutoGrid Alignment Tool (FEI, Part-No. # 9432 909 97641; described below)
- CryoFIB AutoGrid (FEI, Part-No. # 1149142)
- C-ring (FEI, Part-No. # 9432 909 97551)
- C-ring Insertion Tool (FEI, Part-No. # 9432 909 97571)

- Small screwdriver (to close/open the shuttle clamp)
- Cryo-fluorescence microscope, e.g., CorrSight (FEI) or cryo CLEM (Leica)
- Cryo-transmission electron microscope where AutoGrids can be loaded, e.g., Titan Krios or other FEI microscope with Autoloader, Polara microscope with the modified cartridge or modified side entry holder

Software

- xT user interface and server v13.4.2 (Thermo Fisher FEI)
- MAPS v3.6 (Thermo Fisher)

Reagent Setup

- ***Complete DMEM*:** Prepare DMEM containing 10% (vol/vol) HyClone Bovine Calf Serum and 1% (vol/vol) HyClone Penicillin-Streptomycin. Complete DMEM can be stored at 4 ° C for a few months.
- ***50 µg/ml Fibronectin Bovine Plasma*:** Prepare a 50 µg/ml Fibronectin Bovine Plasma solution in DMEM. Prepare aliquots according to the protocol provided by the manufacturer; aliquots can be stored at – 80 °C for at least one year.

Equipment Setup

- ***Environmental setup:*** To minimize the impact of relative humidity on the ice contamination on specimens, cryo-sample preparation/handling and microscope operation should be performed in the environmentally controlled room (~21 °C and the relative humidity level at 30 % or less). If this is not possible, dehumidifiers can be used to decrease the humidity of the room. Throughout this workflow, N_2 gas is continuously produced through evaporation from LN_2. Installation of a reliable O_2 monitor (e.g., Advanced Micro Instruments, Model 221R) in the confined space is absolutely required and ensure adequate ventilation to avoid asphyxiation.

PROCEDURE

Culturing mammalian cells on gold EM grids ● Timing 70 min to prepare grids, plus 16 – 24 h to culture cells on grids.

1. Prepare adherent mammalian cells in culture to the typical cell density according to the standard protocol for that cell line. The NIH/3T3 cells used as an example in this protocol should be cultured with xx ml complete DMEM in 10 cm cell culture dishes to a confluence of 50 – 80%.
   CRITICAL STEP: Suspension cells should be cultured as a normal suspension culture and can be deposited directly onto copper grids. In this case, proceed directly to Step 12. See the Experimental Design section for additional guidance.
2. Assemble a wet chamber system by placing a filter paper in the cell culture dish so that it covers the whole bottom and wet it with Milli-Q water. Put a sterilized piece of parafilm, slightly bigger than a microscope slide, in the culture dish onto the filter paper. This chamber is used to prevent the fibronectin solution on the grids from drying out during incubation (see Step 5).
3. Place gold EM grids on a sterilized microscope slide glass with the carbon side upwards.

4. Glow discharge the EM grids according to the manufacturer's instructions.
5. Immediately after glow discharging, apply 10 – 20 µl of a 50 µg/ml fibronectin solution on the grids from the side. If the grids float, gently push them down on their edges with tweezers to make sure they are covered under the solution. Place the microscope slide into the wet chamber system from Step 2 and incubate it in the 5 % CO_2 incubator for 30 min.
6. Meanwhile, wash the cells twice with 5 ml DPBS without calcium nor magnesium.
7. Detach the cells by incubating with 1 ml Trypsin-EDTA for 2-5 minutes in the cell incubator. Collect the cells with 4 ml complete DMEM and transfer them into a 15 ml conical tube.
8. Centrifuge the cells at 400 x g for 5 min at room temperature and remove the supernatant containing the Trypsin.
9. Resuspend the cell pellet in 2-5 ml complete DMEM and determine the cell concentration with the hemocytometer.
10. Prepare 21 ml cell suspension with warm complete DMEM containing 250,000 to 500,000 cells in a 50 ml conical tube. The required cell concentration should be determined case by case and aim to have approximately one single cell per mesh on a 200 mesh gold EM grid. Verify that cells are well dispersed into single cells. If not, pipette up and down.
11. Transfer the microscope slide with the fibronectin-coated gold EM grids from Step 5 into a new 10 cm culture dish and very gently add the cell suspension from the bottom of the dish to avoid floating of grids.
    CRITICAL STEP It is crucial to add well-mixed cell suspension into the dish containing grids to have a homogenous distribution of cells on the grids.
    [Optional] When numbers of cells or media are limited, fibronectin-coated grids can be placed on the elevated plastic rim of 3.5 mm glass-bottom MatTek dish. In this case, 2 ml of media and much-reduced numbers of cells (25,000 to 50,000) are required for the preparation of the grids with the same density. These systems facilitate one to grab EM grids by a tweezer from culture dishes without excess bending and damaging of EM grids during the following plunging step.
12. Incubate the culture dish in the CO_2 incubator for 16 – 24 h until the cells are attached to the gold grids. Check the attachment state with the light microscope. ?TROUBLESHOOTING
13. [Optional] When using suspension cells, gently pipette them (~5 µl) on the carbon side of glow-discharged copper EM grids. The suitable cell concentration needs to be optimized. See the Experimental Design section for recommendations when adapting the procedure for using bacteria or yeast cells.

Plunge freezing of the sample ● Timing 2 min per EM grid, plus 10 minutes preparation and 10 minutes cleanup

14. In order to retain the pH and temperature of the media during the plunging procedure, add 1 M HEPES pH 7.4 solution to the culture media at 20 mM final concentration and keep dishes on the 37 °C heat block.
15. Plunge-freeze the cells using a standard or optimized protocol for either a homemade or commercial plunge freezers like Vitrobot or CP3[47]. For cellular blotting, we routinely perform one side blotting from the non-cell side. The blotting parameters have to be optimized.
    ! CAUTION Use personal protective equipment such as safety glasses, face shield, and cold-resistant gloves when working with liquid N_2 to avoid frostbite.
    CRITICAL STEP Optimal cell concentration and blotting time have to be determined for each sample.

PAUSE POINT The frozen sample can be stored for up to several months in liquid N_2 inside a storage dewar.

Sample clipping ● Timing 4 min per EM grid, plus 10 minutes set up and 10 minutes cleanup

16. In order to align the sample correctly in the Cryo-FIB shuttle for cryo-FIB milling and in the Titan cassette for cryo-ET, before clipping, mark the AutoGrid by felt-tip pen (**Fig. 2**).
    CRITICAL STEP It is critical to mark a conventional AutoGrid due to the lack of embedded marks.
17. Place the metal AutoGrid Alignment Tool in the preparation base (**Fig. 5a**) and fill it with clean liquid N_2. Always cover the preparation base when not filling or using it.
    ! CAUTION Use personal protective equipment such as safety glasses, face shield, and cold-resistant gloves when working with liquid N_2 to avoid frostbite.
    CRITICAL STEP Use a surgical mask when manipulating the sample in liquid N_2 to reduce contamination from breath. Always dry tools before re-use to minimize condensed-ice contamination on the grid. An illuminated magnification device is helpful for the following steps.
18. Insert a FIB-AutoGrid with the flat side facing down into the designated cavity in the AutoGrid Alignment Tool.
19. Transfer a grid box containing the plunged grids from Step 14 into the preparation base using pre-cooled large tweezers (**Fig. 5a**).
20. Open the grid box using the pre-cooled tool and place a sample EM grid into the FIB-AutoGrid. Orient the EM grid in the FIB-AutoGrid with the cell side facing down to allow for subsequent milling (**Fig. 2**).
21. Load a C-ring into the C-ring Insertion Tool. Use tweezers to insert the C-ring into the tool's tip. Press the C-ring Insertion Tool on a flat, firm surface and gently push the C-ring in order to align it with the tooltip rim.
22. Insert the loaded, pre-cooled C-ring Insertion Tool vertically into the AutoGrid Alignment Tool and place it on the sample containing FIB-AutoGrid.
23. Gently push the C-ring down to clip the sample EM grid into the FIB-AutoGrid. Turn the FIB-AutoGrid upside down and back to ensure that the grid is clipped correctly.
    CRITICAL STEP The use of excessive force when pushing the C-ring down may cause the breakage of the Quantifoil. Therefore, be gentle in this step.
    PAUSE POINT If storing for later use, transfer the clipped sample into the AutoGrid box and close it using the pre-cooled tool. The sample can be stored for up to several months within liquid N_2 in a storage dewar.

[OPTIONAL] Cryo-fluorescence microscopy for cryo-CLEM● Timing 1-5 hours based on instruments to be used and the numbers of grids to be observed.

24. When the proteins, organelles, or cells of interest are fluorescently labeled, homemade or commercially available fluorescence microscopes equipped with cryo-stage such as CorrSight (FEI), cryo CLEM (SP8 Leica) are used for localization of these structure within EM grids. The detailed protocol for such a procedure is previously published[47]. The obtained fluorescence images are used for targeted cryo-FIB milling and subsequent cryo-ET data acquisition (see below steps 60 and 104).

Cooling down the microscope ● Timing 20-30 min

25. Ensure that the microscope chamber pressure is ~ $1\text{-}3\times10^{-6}$ mbar at room temperature (~ 21

°C) before cooling.
CRITICAL STEP For shared instruments, verify that samples are removed before cooling the microscope. If the microscope is already cooled down and the samples cannot be transferred through the quick loader, the microscope has to be warmed up before venting, and then pumped again for several hours before starting cooling down.

26. Open the N_2 gas flow for both the shield and the stage at the flow control to the maximum level of 10 l min^{-1}.
CRITICAL STEP To eliminate any trace of water within the N_2 gas carrying lines, start this step well in advance before inserting the heat exchanger into the liquid N_2 dewar. The traces of water, if not removed, would turn to ice crystals when the cryo-cooled N_2 gas begins flowing, and the crystal would impede the seamless flow of cryo-cooled N_2 gas.
27. Make sure that the vacuum pump for evacuating the insulating hoses shielding the cold N_2 gas carrying lines is on (**Fig. 4b**).
28. Fill the heat exchange dewar with liquid N_2 (**Fig. 4a-b**).
! CAUTION Use personal protective equipment such as safety glasses, face shield, and cold-resistant gloves when working with liquid N_2 to avoid frostbite.
29. Start the temperature log software to monitor the cooling process.
CRITICAL STEP Start the temperature log software just before inserting the heat exchanger to use the timer for controlling the cooling liquid N_2 level in the dewar. The liquid N_2 dewar (**Fig. 4b**) will cool the setup for approximately 8-10 h, and continuous monitoring of the temperature is advised.
30. Slowly insert the heat exchanger into the previously filled liquid N_2 dewar and ensure that it is properly inserted (**Fig. 4b**). There is a small cup at the bottom of the dewar; the heat exchanger should sit well into this cup.
CRITICAL STEP Do not hold the heat exchanger by the hoses of the N_2 gas as it may damage the hoses. Hold the heat exchanger only by its metallic handle.
31. After the temperature has stabilized to ~ - 180 °C, adjust the N_2 gas flow for the shield and the stage to get a better cooling result of ~ - 183 °C (usually ~ 8.5 l min^{-1}). The pressure in the microscope chamber should reach down to $4\text{-}7\times10^{-7}$ mbar. This drop in pressure is brought by the cryo-shield and stage (now at cryo temperature) trapping gaseous particles inside the microscope chamber.
CRITICAL STEP The temperature sensor of the stage of Aquilos is attached to the lower stage, and the upper stage where the shuttle is inserted are connected via a cryo-bearing. Considering the thermal conductivity via cryo-bearing and mass of the upper stage, we recommend loading samples at least 30 min after the stage temperature reaches at -180 °C.
CRITICAL STEP Note that under normal usage conditions, accumulation of dust and sputtered/deposited Platinum compromises thermo-conductivity between the lower and upper part of the cryo-stage. Even though the temperature of the lower stage is shown to be less than 180 °C, we routinely measure the temperature of the upper stage and shuttle with thermocouples and inspect/clean cryo-bearing in case of compromised cooling of them.
? TROUBLESHOOTING

Sample loading ● Timing 10-20 min

32. Always make sure that the transfer rod (**Fig. 6a**) and the preparation base (**Fig. 5a-c**) are dry and clean before using. Place the shuttle in the preparation base (use latex/nitrile gloves) and check for the shuttle clamp to be in the open position (**Fig. 5b**)

! CAUTION Always use gloves to handle the shuttle to avoid exposure to any toxic materials from the shuttle and to prevent the accumulation of any possible impurities from the hands onto the shuttle.

CRITICAL STEP It is recommended to keep the dry transfer rod closed and under vacuum conditions between uses, for which the transfer rod can be kept attached to the quick loader.

33. Open the N_2 gas flow for the transfer rod lid and box shortly before use to flush them with N_2 gas (**Fig. 5c, e**).
34. Fill the preparation base with clean liquid N_2 until the shuttle is fully covered. Always cover the preparation base with standard lid (not shown) when not filling or loading (**Fig. 5a**).

! CAUTION Always use personal protective equipment such as safety glasses, face shield, and cold-resistant gloves when working with liquid N_2 to avoid frostbite.

35. Transfer an AutoGrid box containing the clipped samples into the preparation station box using pre-cooled large tweezers.
36. Open the AutoGrid box with the pre-cooled tool and load the clipped samples with pre-cooled tweezers into the shuttle. The cells are located on the flat side of the FIB-AutoGrid (Fig. 3b). This flat side is the side to be milled and must face outwards from the shuttle and towards the clamp (Fig. 4). Orient the AutoGrid with the milling slot pointing toward 12 o'clock to be in line with the ion beam later. The two samples in two AutoGrid can be loaded simultaneously in the shuttle (**Fig. 3a**).

! CAUTION Use personal protective equipment such as safety glasses, face shield, and cold-resistant gloves when working with liquid N_2 to avoid frostbite.

CRITICAL STEP Use a surgical mask when manipulating the sample in liquid N_2 to reduce contamination from breath. Furthermore, dry the tools before re-use to minimize ice contamination on the grid.

37. Tighten the shuttle clamp by turning a shuttle clamp knob (**Fig. 5b**). By gently tilting shuttle, verify both grids are properly held by the clamp. Flip the shuttle 90° into the transfer position and attach the transfer rod lid. Make sure the sliding valve of the preparation base is closed (Fig. 5c).
38. Detach the transfer rod from the quick loader of the microscope by pushing the V button in the Vaccum control buttons (**Fig. 6b**) and attach it on top of the transfer rod lid (Fig. 5d). Confirm that the transfer rod slider lever is locked, the shuttle grabber locked (which will hold the shuttle) is unlocked, and the transfer rod valve is closed (**Fig. 6a, c, d**).
39. Pump transfer rod lid chamber by pushing the "Pump" button in the Transfer rod control panel (Fig. 5e) for 30 seconds, open transfer rod valve (**Fig. 5d**), and vent by pushing the "Vent" button in the Transfer rod control panel.
40. Open the sliding valve of preparation base, unlock the transfer rod slider lever, and carefully insert it into the shuttle (**Fig. 5d**), then lock the shuttle grabber lock.

CRITICAL STEP The transfer of the shuttle into the microscope chamber takes place under a poor vacuum and without active cooling. The following steps have to be performed quickly.

41. Pull the transfer rod with the attached shuttle back and lock the transfer rod slider lever.
42. Close the sliding valve of the preparation base and pump the lid chamber attached with the transfer rod for 30 - 40 seconds.
43. Close the transfer rod valve and vent the lid chamber with N_2 gas.
44. Detach the transfer rod, transfer and attach it to the quick loader system of the microscope (**Fig. 6b**).
45. Start pumping the quick loader by pushing the "P" button. The stage moves to the loading

position.

46. When the quick loader is pumped ("OK" button flashes), open the valve to the microscope chamber and, subsequently, the transfer rod valve (**Fig. 6b**).
47. Unlock the transfer rod slider lever and insert it all the way into the microscope to mount the shuttle onto the stage.
48. Unlock the shuttle grabber lock to release the shuttle, pull the transfer rod back and lock the transfer rod slider lever while verifying the shuttle is no longer attached on the transfer rod.
49. Close the valve to the microscope chamber and the transfer rod valve.
    CRITICAL STEP The transfer rod could remain attached to the quick loader system under vacuum conditions during milling. The transfer rod in this condition is ready for sample retrieval (**Fig. 6b**).
50. Discard the liquid N_2 and dry the preparation base for re-use.

Acquiring tile-set of the grid and identifying milling targets ● Timing 30 min

51. [Optional] When using an Aquilos system, visually navigate the stage position after taking an overview image of the stage with a CCD camera (Nav-Cam). Refer to Box 1 describing key operations with the xT software (used for controlling microscope).
52. Set the electron and ion beam setting and data acquisition settings, as shown in Tables 1 and 2.
    CRITICAL STEP If not milling, always use the ion beam with the lowest possible current to minimize radiation damage to the sample.
53. Open the cryo-control panel in the xT software, choose the grid (grid 1or 2) and move the stage to the mapping position at which the stage tilt would be 45°.
54. [Optional] When using older Scios versions, the cryo-control and preset Mapping position may not be available in some versions of the xT user interface. For such cases, move the stage to position X: 0.0 mm, Y: 0.0 mm without changing the Z coordinate and then move the stage to the center of one of the grid and focus. Link the stage to Z and move the stage to bring Z to the free working distance of 7 mm. Refer to Box 1 for details about linking the stage.
    CRITICAL STEP Linking the stage ensures proper coordinate calibration and thus prevents the accidental clashing of the shuttle with the hardware of the columns.
55. Begin SEM and FIB imaging at low currents to update the SEM and FIB view with the latest images, adjust the focus of the both the SEM and FIB views, and apply scan-rotation (180°) to both the views. The sample can be checked and validated, e.g., cell concentration and distribution, ice thickness, and holey carbon layer integrity.
    ? TROUBLESHOOTING
56. Start the MAPS software available with the Aquilos system (Refer to Box 2) and create a new project in the MAPS.
57. Acquire a snapshot of the whole grid in the MAPS.
58. Create, design, and position a tile-set to cover a large area of EM grids. Update the focus property of the tile-set to match the focus value adjusted in step 55 in the xT user interface.
59. Start the tile-set acquisition by clicking the play button in the bottom-most panel of the MAPS interface. It will take some time based on the properties & parameters of the tile-set.
    CRITICAL STEP Do not make changes on the xT user interface as the MAPS should have the control of the dual-beam microscope during the acquisition of the tile-set.
60. [Optional] Integrate light microscopy images for target milling for specific cells and region of cells using MAPS (Box 2). Any fluorescence images (from Step 24) can be uploaded into the

existing MAPS project to perform correlation (Refer to Box 2).

61. Search over the entire high-resolution tile-set to identify a spot where the milling is intended (milling spot). The milling spot should be within a ~ 600 µm (~ 5 meshes on a 200-mesh EM grid) radius around the grid's midpoint (**Fig. 2b**) to ensure that the lamella can be used for Cryo-ET. Choose relatively small cells to ensure vitreous conditions inside cells, and the carbon support layer must be intact to prevent instability during the grid transfers.
    ? TROUBLESHOOTING
62. Go to the milling spot, right-click and choose 'add a lamella site' to create a new lamella layer in the MAPS for this milling spot. Give this lamella layer a well-identifying name.
63. Place milling spot at the Eucentric height (**Fig. 4d**) by using the 'Calculate Eucentricity' tool of the MAPS software and drive the stage to the Eucentric position by clicking the 'Drive to' button right next to the Eucentric position property.
    CRITICAL STEP When performing Eucentric positioning without MAPS, turn on the live acquisition of the SEM images at a given tilt angle. Tilt the stage by few degrees. If the current Z is not at the Eucentric height, then the SEM view area will shift when the stage is tilted. Adjust the Z height till the image shift in the SEM view is minimized.
64. Precisely identify the milling spot in both the SEM/FIB views, determine the best tilt angle for the milling, and set/update the tilt angle in the milling position property of this milling spot. Choose the milling angle based on the sample thickness (**Fig. 7b**).
    ? TROUBLESHOOTING
    CRITICAL STEP The X Y Z (Eucentric height) and T (tilt angle of milling) values determined for the milling spot can be stored in xT user interface with an appropriate identifying name in the stage control panel.
65. Repeat the Steps 61-64 for all the different milling spots to complete the design of the entire milling process.

Sample milling ● Timing 45 – 90 min per lamella

66. For the Pt Deposition through GIS (**Fig. 7a**), open the cryo-control panel in the xT user interface, choose the grid (grid 1or 2) and move the stage to the Pt deposition position which is a preset position, specifically designed for the Pt deposition on the selected grid.
    If the MAPS is being used, then a majority of the microscope operations would be controlled by MAPS. Therefore, acquire the GIS needle control (from MAPS) by choosing the GIS deposition option in the dropdown list of the Microscope option of the MAPS' toolbar.
    CRITICAL STEP If not using MAPS and cryo-control panel, the GIS stage position and length have to be pre-determined by users prior to the experiments.
67. Open the patterning panel in the xT user interface. Insert the GIS needle and open the GIS for deposition for 6-9 s. After deposition, take an SEM overview image to verify the deposition. The thickness and uniformity of the platinum layer can be regulated by deposition time, GIS temperature, the distance between the GIS needle and the grid(s). 6-9s of deposition time in the preset Pt deposition position at GIS temperature of 28° should lead to the layer of one to three micrometers in thickness. The thick GIS layer significantly obscures the sharp topological features of the sample surface, making it difficult to identify cell(s) and their shapes. Therefore milling spots determination has to be done prior to organoplatinum (GIS) deposition.
68. Go back to the pre-registered milling position by MAPS. The following milling process has to be under the xT user interface.

69. Before start milling, bake the sample by FIB imaging. This imaging causes the release of volatile organic components from the organoplatinum deposition (**Fig. 7a**). The initial FIB image drift is gradually stabilized while the release proceeds.
70. Open the patterning panel in the xT user interface. The example of a milling pattern is shown (**Fig. 7c**). The milling patterns can be saved as presets, or they can be saved as files. To load the milling patterns, either select the preset or import the milling pattern file. Position the loaded rectangular milling patterns and start the rough milling with 300 – 1000 pA.
    CRITICAL STEP The width of the lamella (e.g., 2/3rd of cellular width) should be significantly smaller than that the cell width to leave the surrounding cellular structure as a support for the lamella.
    ? TROUBLESHOOTING
71. Continuously monitor the evolution of the lamella in the SEM and FIB views (Table 1 and 2). An SEM view update can be set up in the iSPI section of the patterning control by specifying the duration of the update (E.g., every 10 s).
    CRITICAL STEP The excess imaging could significantly compromise the sample integrity, which would only be visible later in subsequent TEM observation. Try to minimize unnecessary SEM and FIB imaging of lamellae, particularly toward the end of milling steps.
    ? TROUBLESHOOTING
72. After finishing the rough milling, bring the milling patterns closer together and continue milling with a lower ion beam current (e.g., 100 pA) (**Fig. 7c**). As the material is milled away, jointly adjust the milling patterns and the ion beam current to get to the desired lamella thickness.
    ? TROUBLESHOOTING
73. For the last milling step, position the patterns to precisely define the lamella shape and polish the lamella with an extremely low ion beam current (10 – 30 pA).
    ? TROUBLESHOOTING
74. Repeat Steps 66-73 above to generate a lamella for all the identified milling spots.
    ? TROUBLESHOOTING
75. The exposure of the lamella surface for several hours inside the microscope chamber significantly results in the deposition of material on the lamella surface. Perform short surface cleaning of all lamellae with an extremely low ion beam current (10 – 30 pA) just before retrieval.
    ? TROUBLESHOOTING

Platinum sputtering (optional step, only available in some microscopes) ● Timing 5 min
CRITICAL Platinum sputtering is the process by which platinum atoms are ejected from its source by high energy plasma for its thin-layer deposition onto a sample. This thin-layer (usually 5 nm-50 nm) adds a conductive layer to the sample and prevents the build-up of electron or ion-beam charges. This layer can be deposited prior to milling (pre-milling) for better SEM-FIB imaging/milling and post-milling (for deposition onto lamellae) for better TEM imaging. The latter is highly recommended if phase-plates are to be used in TEM for improving contrast; since the conductive layer (~ 5nm thick) prevents the build-up of charges and thus a potential across the lamellae which can affect phase-plate assisted TEM imaging. Since the GIS deposition of organic platinum also improves sample conductivity; the use of platinum sputtering prior to milling is not critically necessary, but is recommended if the dual beam is equipped with a

platinum sputterer. The steps of platinum sputtering, described ahead, is principally similar for pre/post-milling.

76. Open the cryo-control panel in the xT user interface, under the sputter coating settings, click 'Prepare for sputtering' button to drive the stage into the position for sputtering. 'Prepare for sputtering' button will change to 'Recover from sputtering' button.
77. Specify the current, voltage, pressure of the surrounding Argon gas, and run-time of the plasma generation and sputtering. These parameters determine the thickness of the Platinum deposition. A thickness of ~50 nm/5nm is recommended for pre/post-milling sputtering respectively.
    CRITICAL STEP Note that, instead of specifying all the parameters each time, a preset can be set, stored and used each time (available as numbered buttons in the sputter coating settings).
78. Choose a preset and then click the run button to begin sputtering.
79. The sputtering will end automatically (when the run button becomes clickable again). Click 'Recover from sputtering' button to bring the stage to the position before sputtering.

Sample retrieval ● Timing 5 min

80. Ensure that the preparation base is completely dry and clean and that the shuttle base in the preparation base is in the receiving position.
81. Fill the preparation base with liquid N_2 as described above, attach the transfer rod lid and close the sliding valve of preparation base.
82. Open the N_2 gas flow for the transfer rod lid shortly before use to flush them with N_2 gas.

At the dual beam microscope

83. Turn off both beams before sample retrieval.
84. Ensure that the transfer rod slider lever is locked, and the shuttle grabber lock is unlocked.
    CRITICAL STEP The transfer of the shuttle back to the preparation station takes place under a poor vacuum and without active cooling, therefore perform the following steps quickly.
85. Pump the quick loader by pushing the "P" button. The stage starts moving to the loading position.
86. When the quick loader is pumped ("OK" button flashes), open the valve to the microscope chamber and, subsequently, the transfer rod valve.
87. Unlock the transfer rod slider lever and insert it all the way into the microscope to grab the shuttle.
88. Lock the shuttle grabber lock, pull the transfer rod back and lock it.
89. Close the valve to the microscope chamber, then the transfer rod valve.
90. When the pressure within the microscope chamber has stabilized the "V" button flashes, press it to vent the quick loader system, transfer and attach the transfer rod to the transfer rod lid.
91. Pump the transfer rod lid chamber for 30-40 s, open the transfer rod valve and flush with N_2 gas.
92. Open the sliding valve of preparation base, unlock the transfer rod slider lever and insert the shuttle into its station.
93. Unlock the shuttle grabber lock and remove the transfer rod and the transfer rod lid.
94. Orient the shuttle in the horizontal position and open the shuttle clamp and transfer the milled sample into an AutoGrid box.
    PAUSE POINT The sample can be stored for several months within liquid N_2 in a storage dewar.
95. Discard the liquid N_2 and dry the preparation base for re-use. Also, ensure that the transfer rod

is dry and evacuated for re-use.

96. Repeat Steps 25-95 for another round of milling.

97. At the end of the session, close the N_2 gas flow for the transfer rod lid and box.

CRITICAL STEP It is highly recommended that the shuttle is immediately baked for an hour in a baking chamber kept in the chemical hood to prevent releasing toxic GIS and Pt coating materials from the shuttle (E.g., organoplatinum). If cleaning is required, the shuttle must be cleaned with lint-free wipes only.

Warming up the microscope ● Timing 30 min

98. At the end of the milling session, set both beams to sleep state and open the N_2 gas flow for both the stage and the shield to the maximum.

99. Take out the heat exchanger and warm up the microscope until the temperature for both the stage and the shield is > 10 °C.

! CAUTION Use personal protective equipment such as safety glasses, face shield, and cold-resistant gloves when working with liquid N_2.

? TROUBLESHOOTING

100. Stop the PicoLog (temperature tracking) program, save the file, and close the software.

101. Lower the N_2 gas flow for the stage and the shield at 1 liter/min to keep N_2 gas carrying lines to be dry and clean.

Loading the sample for cryo-ET ● Timing 20 min

102. The loading procedure of the AutoGrids should be performed according to the manufacturer's protocol. Load the milled grids into the Autoloader cassette, orienting the grids such that the lines parallel to the milling direction would be perpendicular to the tilt axis during cryo-ET. To achieve this, the mark on the rim of the AutoGrid (shown in blue in **Fig. 2** below) should appear centered to the user in a perfect (90°) top-down view.

103. While maintaining the above orientation of the grid, carefully load the AutoGrids into the cassette. Utmost care must be taken to ensure that the grid's orientation does not change.

Tilt series data collection● Timing several hours to days (based on the numbers of samples)

CRITICAL After finding lamellae at very low magnification, we are using SerialEM at low dose mode[85,86] for taking overview images of lamellae and setting up semi-automatic tilt series data acquisition.

104. When correlation with fluorescence image (FM) data is required for the cryo-ET acquisition, create an overlay of FM images (obtained in Step 24) and overview images of grids/lamellas using Fiji using Multi-point and Landmark correspondences available as plugins or MAPS at Aquilos by importing TEM overview saved as 8-bit tif data.

CRITICAL STEP MAPS software operatable at Titan Krios is commercially available from TFS. The MAPS project created at Aquilos can be directly opened at the Titan instrument equipped with MAPS allow direct correlation of FM, SEM, and TEM data and navigation of stage position at Titan Krios.

? TROUBLESHOOTING

105. Determine the pre-tilt angle and its orientation of lamellae by finding the longest and thinnest lamella view by tilting the TEM stage.

CRITICAL STEP: Due to the milling geometry, the lamellae are pretilted to the surface of the EM grid. Thus, at the nominal 0° tilt of the TEM state, lamellae are already tilted based on the

milling angles used during cryo-FIB milling.
? TROUBLESHOOTING

106. In order to maximize the acquisition of high-resolution information at lower tilt angles, we routinely collect tilt series using a dose-symmetric scheme[87].
CRITICAL STEP: The pixel size and tilt angle increment should be pre-determined depending on the purpose of the projects, target-resolution, lamella thickness, and total electron dose.
? TROUBLESHOOTING

Tomogram reconstruction● Timing several hours to days (based on the numbers of samples)

107. Reconstruct tomograms using conventional software and protocols. We are routinely using patch tracking of Etomo from IMOD[85,86,88].
? TROUBLESHOOTING

Timing

This protocol can also be performed stepwise over several days. After each step of sample plunge freezing, clipping, and cryo-FIB milling, the grids can be stored in liquid N_2 for several months. The specific timing information given below refers to a practiced user; new users may need more time for each step.

Steps 1-13, Culturing mammalian cells on gold EM grids: 70 min to prepare grids, plus 16 – 24 h to culture cells on grids.

Steps 14-15, Plunge freezing of the sample: 2 min per EM grid, plus 10 minutes preparation and 10 minutes cleanup.

Steps 16-23, Sample clipping: 4 min per EM grid, plus 10 minutes set up and 10 minutes cleanup

Step 24 (Optional) Cryo-fluorescence microscopy for cryo-CLEM: 1-5 hours

Steps 25-31, Cooling down the microscope: 20-30 min

Steps 32-50, Sample loading: 10-20 min

Steps 51-65, Acquiring tile-set of the grid and identifying milling targets: 30 min

Steps 66-75, Sample milling: 45 – 90 min per lamella

Steps 76-79, Platinum sputtering (optional step, only available in some microscopes): 5 min

Steps 80-97, Sample retrieval: 5 min

Steps 98- 101, Warming up the microscope: 30 min

Steps 102-103, Loading the sample for cryo-ET: 20 min

Steps 104-106, Tilt series data collection: several hours to days (based on the numbers of samples)

Step 107, Tomogram reconstruction: several hours to days (based on the numbers of samples)

Troubleshooting

Troubleshooting advice can be found in Table 3

Anticipated results

Following this protocol, a cryo-EM knowledgeable user can prepare lamellae suitable for high-resolution cryo-ET and image processing (**Fig. 8**). The target lamella thickness should be determined based on the project aims and target resolution. Some issues occurring during the workflow can usually only be detected when the sample is loaded in TEM. Common problems are breaks or cracks in the holey carbon support layer (**Fig. 9a**), broken lamellae, lamellae with heterogenous thickness (**Fig. 9b**), presence of non-vitreous ice in the lamellae (**Fig. 9c**), crystalline ice, and de-vitrified ice (has leopard skin-like appearance) (**Fig. 9d**). The required optimization of the workflow in case of these problems is discussed in detail in the troubleshooting section (Table 3).

Table 1 | Beam settings for SEM and FIB for frozen biological samples

	Voltage (kV)	Current (pA)	Detector	Mode
SEM	2-5*	25	ETD	Standard
FIB	30	1.5**; 10-500***	ETD	Standard

*Contrast difference between 5 and 2 kV SEM images can be used to gauge lamellae thickness **and *** for live imaging and active milling purposes, respectively.

Table 2 | Image acquisition settings for SEM and FIB during sample preparation

	Live (FIB/SEM)	Snapshot (SEM only)	Photo (SEM only)
Dwell Time	200 ns	200 ns	1 to 2 µs
Line integration	1	1	1
Resolution	1536 x 1024	3072 x 2048	6144 x 4096
Bit Depth	8	8	8

A live feed is used to monitor the milling process at FIB and SEM view. For the recording purposes of milling, SEM/FIB image snapshot setting is used. Photo setting is used only for recording purpose of low2 magnification image covering a whole grid due to the high electron dose. FIB imaging should be minimized due to the non-targeted sample damaging by FIB.

Table 3 | Troubleshooting table

Step	Problem	Possible reason	Solution
5	All the grids have floated.	Glow discharge is not sufficient to cause enough hydrophilicity, or grids are not used within a suitable time (30 min) after the glow discharge.	Glow discharging of grids should be done within 30 min before usage. Verify grow discharge condition.
12	The cells do not adhere properly.	Glow discharging is not sufficient. The cells need another type of extracellular matrix or higher density	See above. Optimize cell culture conditions.
31	Cryo-stage/Cryo-shield temperatures rise significantly above -170 °C	N_2 gas flow for cryo-shield and cryo-stage decreases significantly lower than needed.	Adjust the N_2 gas flow at the source. If the same source of N_2 gas is used for both the preparation station and cooling the cryo-stage, the prolonged use of N_2 gas at the preparation station (e.g., for drying the preparation station) may sequester some

			N_2 gas and reduce its flow rate into the cryo-stage and cryo-shield. A leak of cold N_2 gas inside/along the heat exchanger. Check all the tubing connections. Unusual frost observed in the heat exchanger often indicates a location of cold N_2 gas leak.
57 & 59	Ice contamination on top of the sample before milling	Contaminated liquid N_2 during plunge freezing, clipping, and sample loading If the samples are observed by cryo-fluorescence microscopy, some degree of contamination should be accepted. Vacuum issues during the transfer	Reduce room humidity Dry liquid N_2 dewars before filling with fresh liquid N_2 Filter liquid N_2 with coffee filters Wear a mask to prevent contamination from the breath Carefully dry tools before re-use Check and clean valves and O-rings
57 & 59	Many broken EM grid meshes (Fig. 9a)	Damage during seeding cells on grids, plunge freezing or clipping	Evaporate a thin carbon layer on top of Quantifoil grids using carbon evaporator to make the substrate stronger Consider Quantifoil grids with SiO_2 film known to provide more robust and stiffer support[89].

			Manipulate grids more gently. Careful and gentle clipping, e.g., approach the EM grid in the FIB-AutoGrid with the C-ring Insertion Tool vertically; do not press the C-ring Insertion Tool vigorously onto the FIB-AutoGrid while pushing the C-ring down.
57 & 59	No cells on the EM grid	Insufficient glow discharging of grids Cell concentration too low	Use glow discharged grids within 30 min Optimize parameters for glow discharge system Optimize cell concentration during seeding on the grids
64	When SEM and FIB do not show the spot on the grids even at the eucentric height.	The microscope is not well-aligned.	Reset beam shifts both in SEM and FIB. Use beam shift to adjust digitally. If still not possible, it is highly likely the FIB column position/angle needs to be adjusted mechanically.
70	Identification of cells on grids hindered after Pt Deposition	Thick Pt deposition. Check the thickness by the shape of the shadow of the protruding features. Pt deposition occurs at a slight angle, thus leaving behind a	Lower the Pt deposition time Changing the grid-needle distance.

		shadow for protruding features.	Changing the temperature of the GIS is also, not recommended.
66-73	FIB image moves	GIS Pt layer is not yet cured. Too thick ice on the entire sample Ice contamination along the focused ion beam path. The grid bar is along the FIB beam path. If temporal, it could be due to the change of stage temperature	Use FIB to bake (Fig.8b) Prepare a new sample. Increase the milling angle, if possible. Select a different area for milling. Increase milling angle Check stage temperature.
66-73	Milling takes an extremely long time	Platinum layer is too thick Milling the grid bar	Reduce the thickness of the platinum layer by reducing the application time and/or increasing the GIS sample-to-needle distance Adjust milling position. Get familiar with how grid bars look and stop milling
66-73	Lamella bending/moving while milling	Charging is likely causing the beam-induced movement of the lamella	Apply platinum layer Increase platinum layer thickness Carefully supervise milling process and compensate sample movement with ion beam shifts.

		Shrinkage of the EM grid support film at cryogenic temperatures	Make micro-expansion joints[84]
66-73	Lamella breaks while milling	Lamella too thin Beam-induced movement Shrinkage of the EM grid support film at cryogenic temperatures	Make a thicker lamella See "Lamella moves while milling" Make micro-expansion joints[84]
99	Vacuum pressure failure during the microscope warm-up	As water molecules frozen onto cold surfaces (e.g., cryo-shield) releases upon warming up, the pressure rises	Immediately activate pumping of the Microscope chamber.
104-105	Ice contamination on top of the milled lamellae	Contaminated grids Contaminated liquid N_2 during transfers Vacuum issues during transfer	Reduce contamination during grid preparation See "Ice contamination on top of the sample before milling" Check and clean valves and O-rings
104-105	Curtains	No or too thin platinum layer Crystalline ice on the surface before Pt coating The FIB current too high during milling The materials of significantly different density are present in the biological materials	Increase the thickness of the platinum layer by increasing the application time and/or reducing the GIS sample-to-needle distance Minimize ice contamination

			Use lower FIB current to make smoother lamellae Make sure to complete material milling at each step before proceeding to the next milling.
104-105	The back part of the lamella is significantly thicker than front part (close to Pt layer).		Make sure to complete material milling at each step before proceeding to the next milling. Use different angles (plus/minus 0.5 °) for final milling step[83]
104-105	Crystalline ice in the samples	Sample too thick	Increase blotting time Decrease cell concentration on the grid. If cells are too large for plunge freezing, this protocol might not suitable
104-105	"Leopard ice" on top of the lamellae	Shuttle/Stage temperature issue	Monitor stage top and shuttle temperature with thermocouples. Check the N2 flow of the heat exchanger. Inspect and clean surfaces of the upper and lower part of the cryo-stage and cryo-bearing. Retrieve the prepared EM grid from the microscope chamber

			as soon as possible after milling
106	Sample not aligned with milling direction 90° in regard to the tilt axis	Grids are not well-aligned in the shuttle for dual beam microscopy and/or in Titan cassette	Make sure to mark AutoGrid properly and orient them properly in dual beam and TEM.
106	Beam-induced motion while acquiring tilt series	Charging The lamella is too thin The lamella has cracks	Consider coating lamella with Pt sputter coating Create thicker samples Gentle grid manipulation. See "Lamella bending/moving during milling" "Lamella breaks during milling"
107	Difficulties aligning tilt series	Lamellae are too thick to render good contrast The appearance of crystalline ice inside of samples Unstable Record/Tracking areas	Make thinner samples. See below "Invisible amorphous ice layer on the top and/or the bottom of the reconstructed tomogram" Decrease pixel size Need to increase total electron dose See "Crystalline ice in the samples" Choose suitable area for tilt series acquisition.

			Gentle grid manipulation. See "Lamella bending/moving while milling" "Lamella breaks while milling"
106-107	Invisible amorphous ice layer on the top and/or the bottom of the reconstructed tomogram. The existing of this can be only confirmed by the observation that contaminated crystalline ice particles are not directly located on the biological layer.	Redeposition during milling Contamination in Autoloader in Titan Krios	Perform final fine milling just before retrieval of samples as mentioned in step 71. Perform "Cryo-cycle"

1

BOX 1: xT user interface

The TFS dual-beam microscope is user-managed by a software called xT user interface. A server called xT server manages the flow of information amongst the xT user interface, MAPS (Box 2), and the dual-beam microscope.

- Different user accounts (with different settings) can be created for the xT user interface, which can be useful if users of different disciplines routinely use the microscope.
- Users must inform the xT user interface of the distance (free working distance; FWD) between the sample and SEM column, to prevent any accidental hitting of the sample onto the column(s). This informing process is called linking the Z to FWD and is done by pressing the link Z to FWD button, after focusing on the topmost surface of the sample. After linking, the Z coordinate value reflects the distance between the SEM column and the sample.
- It is recommended to use reduced area imaging for focusing as the continuous live acquisition of the SEM/FIB imaging may cause radiation damages. The reduced area can be positioned over distinct but useless features, e.g., a frost particle.

- END OF BOX 1-

BOX 2: MAPS software

MAPS is a Thermo fisher scientific software for automated acquisition/maintenance of images that can work with different kinds of microscopes (light, dual-beam, and transmission-electron microscopes).

- Images are acquired as tile-set(s), before which the tile-set(s) area is user-drawn, and its properties (e.g., magnification, resolution, focus) are user-defined.
- The MAPS interface has a board called image-navigation area where all the acquired images (usually in separate layers) are displayed. The relative positions of these images and distances between them are to scale.
- Any external images can also be exported. Both the acquired and imported images can be aligned to each other using MAPS' alignment tool. Alignment between two images can be done by selecting 1-2 or 3 common points between the two images. As part of light and electron correlative workflow, such alignments can be used to recognize and target features of interest.
- The MAPS allows the insertion of annotations and other useful features over images in the navigation area. A handy feature for cryo-FIB milling is called lamella site. The template of the lamella site allows semi-automatic calculation of the Eucentric position for a given site. The template can also store stage positions for milling (milling position) and SEM imaging (mapping position) at the site. Storage of such positions allows the user to easily navigate between different target areas of the sample and their tilt-angles.

- END OF BOX 2-

Author contributions statements

FRW, RW, DS, and EV designed the project. FRW, RW, RS, DS, and EV performed the experiments. RS, HP, and EV designed and built components of the system. FRW, RW, DS, and EV wrote the manuscript with input from the other authors.

Acknowledgments

We thank Julia Mahamid at the EMBL, Germany, Bernd Fruhberger at the Nano3 at UCSD, and all Villa lab members for insightful discussions and technical supports. The subtomogram average of ribosome shown in Fig.2 is performed by Robert Buschauer. This work was supported by an NIH Director's New Innovator Award 1DP2GM123494-01. We acknowledge the use of the UC San Diego cryo-Electron Microscopy Facility (partially supported by a gift from the Agouron Institute to UC San Diego) and the San Diego Nanotechnology Infrastructure (SDNI) of UC San Diego, a member of the National Nanotechnology Coordinated Infrastructure, which is supported by the National Science Foundation (ECCS-1542148).

Competing financial interests

EV, FRW, RW, and MS have no competing financial interests. RS, HP, and PF are employees of TFS.

Data availability statement

Cryo-ET representative tomograms have been deposited in the Electron Microscopy Data Bank (EMDB) under accession codes EMD-XXX.

FIGURE LEGENDS

Figure 1

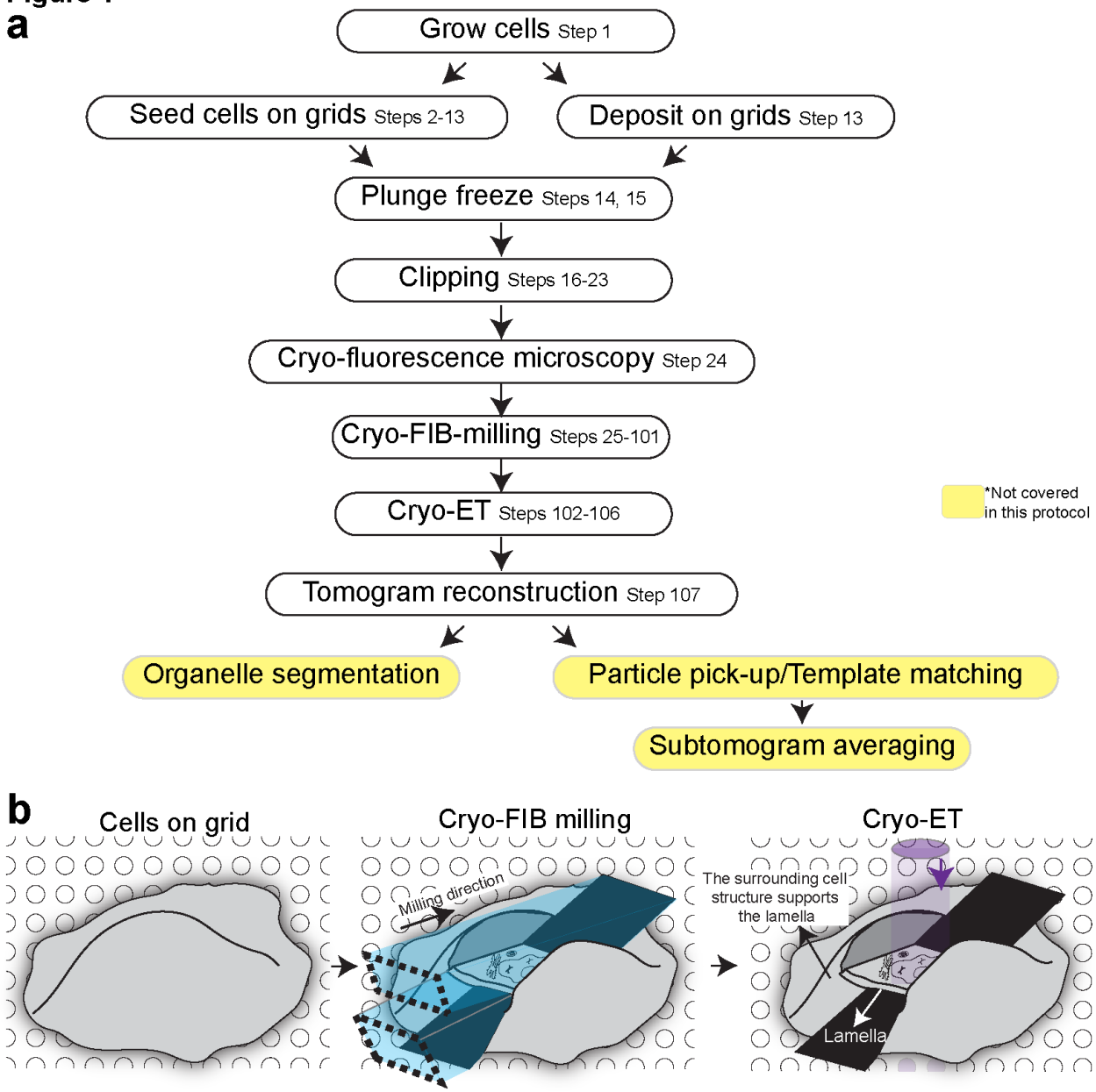

Figure 1| Key steps of the procedure described in the protocol.
a, The cellular tomography workflow. The protocol describes the steps surrounded by black boxes in detail. **b**, Schematic drawing cells on EM grids during workflow.

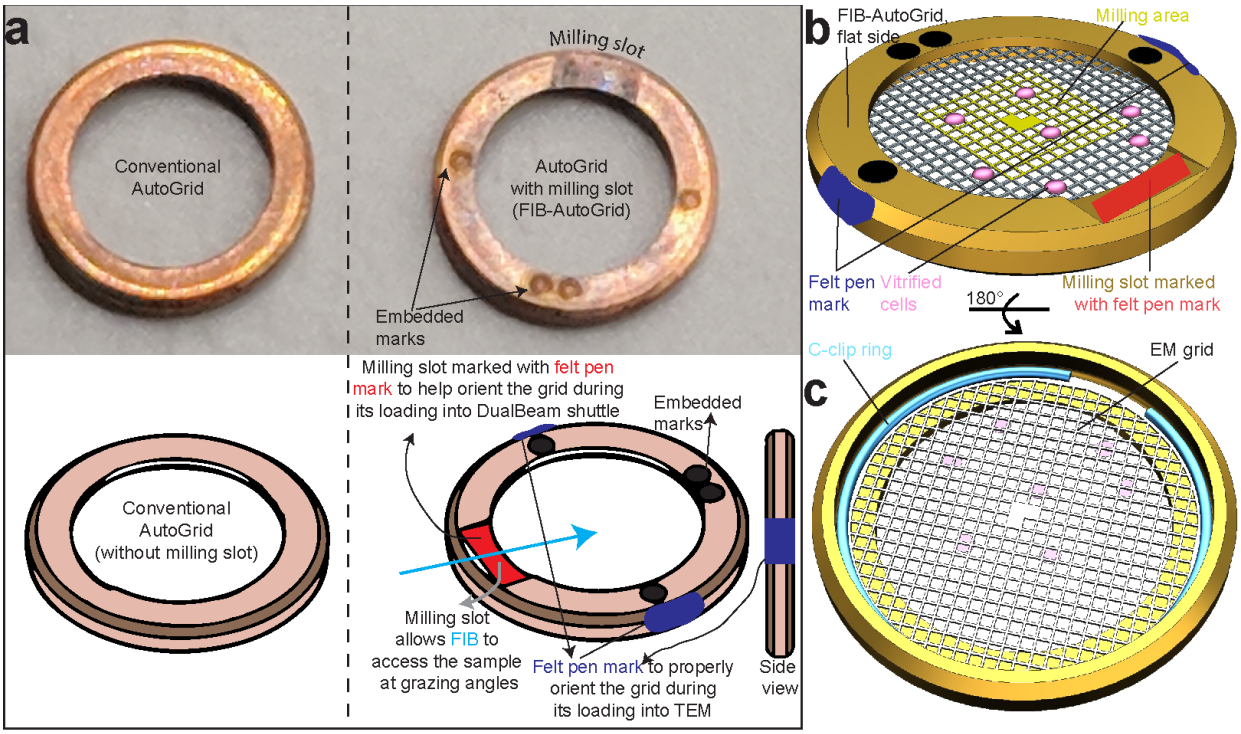

Figure 2| Clipping grids into FIB-AutoGrids.
a, Conventional AutoGrid and FIB-AutoGrid. The milling slots in the FIB-AutoGrids are indicated. To proper adjustment of milling direction and tilt axis during cryo-ET and to increase visibility under liquid Nitrogen, marking using Felt-tip pens prior clipping are required for both conventional and FIB-AutoGrids as shown below. The felt-tip pen mark (red) at the milling slot and blue rim mark enable the orientation of the AutoGrid in the transfer shuttle and Titan cassette, respectively. **b,** FIB-AutoGrid showing the flat side with the modified milling slot. The cells on the EM grid are facing up towards the flat side of the FIB-AutoGrid. The orange square indicates the area for lamella preparation for subsequent cryo-ET. **c**, Back of the FIB-AutoGrid with the EM grid held in place by the C-ring. To allow for subsequent milling, the EM grid is clipped into the FIB-AutoGrid with the cell side oriented down towards the flat side.

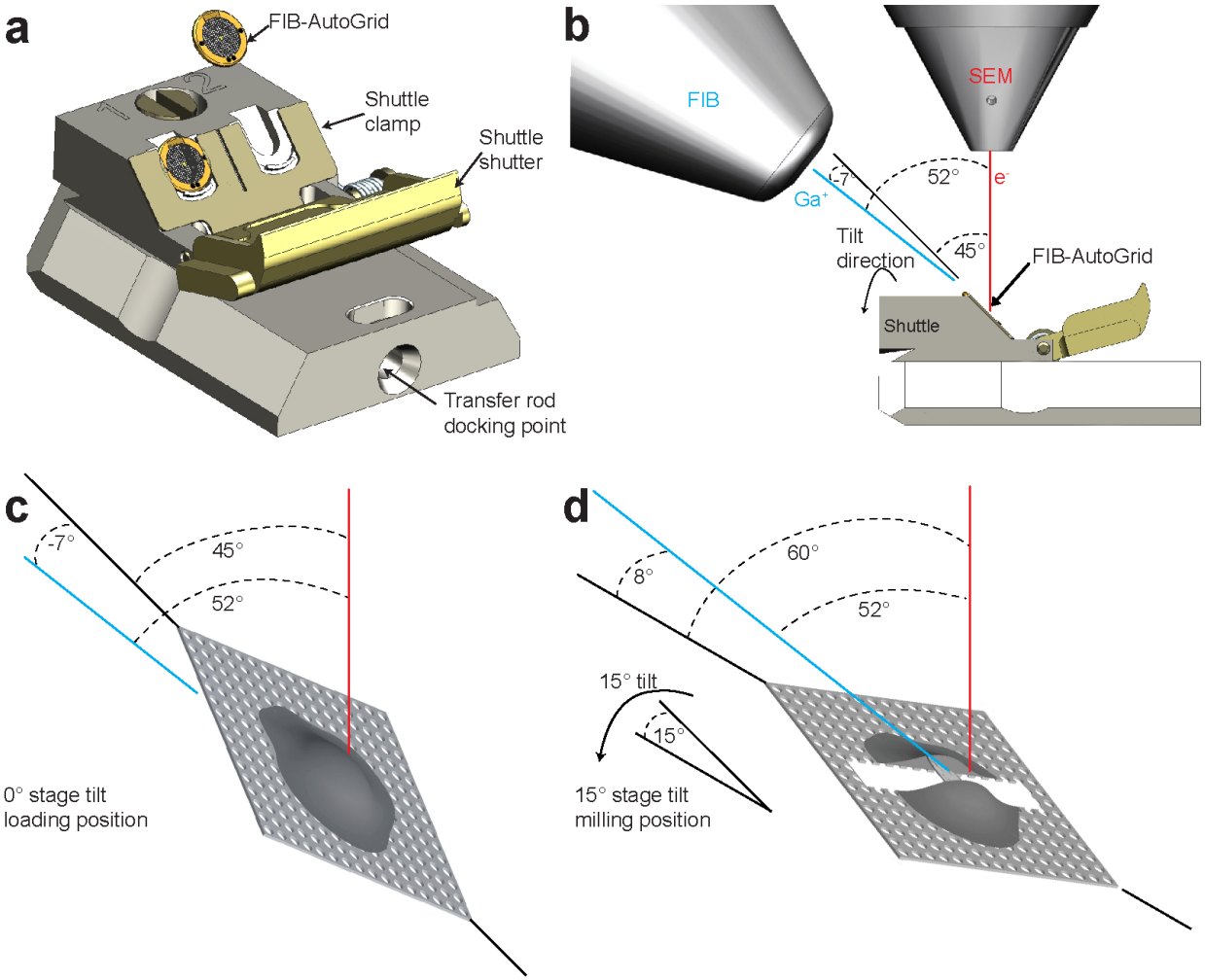

Figure 3| SEM-FIB geometry in dual beam microscopy.
a, The FIB-AutoGrids are placed in the shuttle with the milling slot oriented upwards and the cell side facing outwards. The red felt-tip pen mark at the milling slot facilitates the orientation of the FIB-AutoGrid under liquid N_2. The shuttle is grabbed by the transfer rod at the transfer rod docking point for the transport into the dual beam microscope. **b**, The milling geometry inside the dual beam. The electron and ion beams are placed at 52° from each other. The shuttle is built so that the EM grids are pre-tilted at 45° to the stage surface and the electron beam, and -7° to the focused ion beam. **c, d**, Schematic drawing of a cell attached to the grid loaded inside of dual beam. The shuttle at the 0° stage tilt in **c** and at 15 ° stage tilt in **d**, respectively. Red and blue lines represent electron and galium beams, respectively.

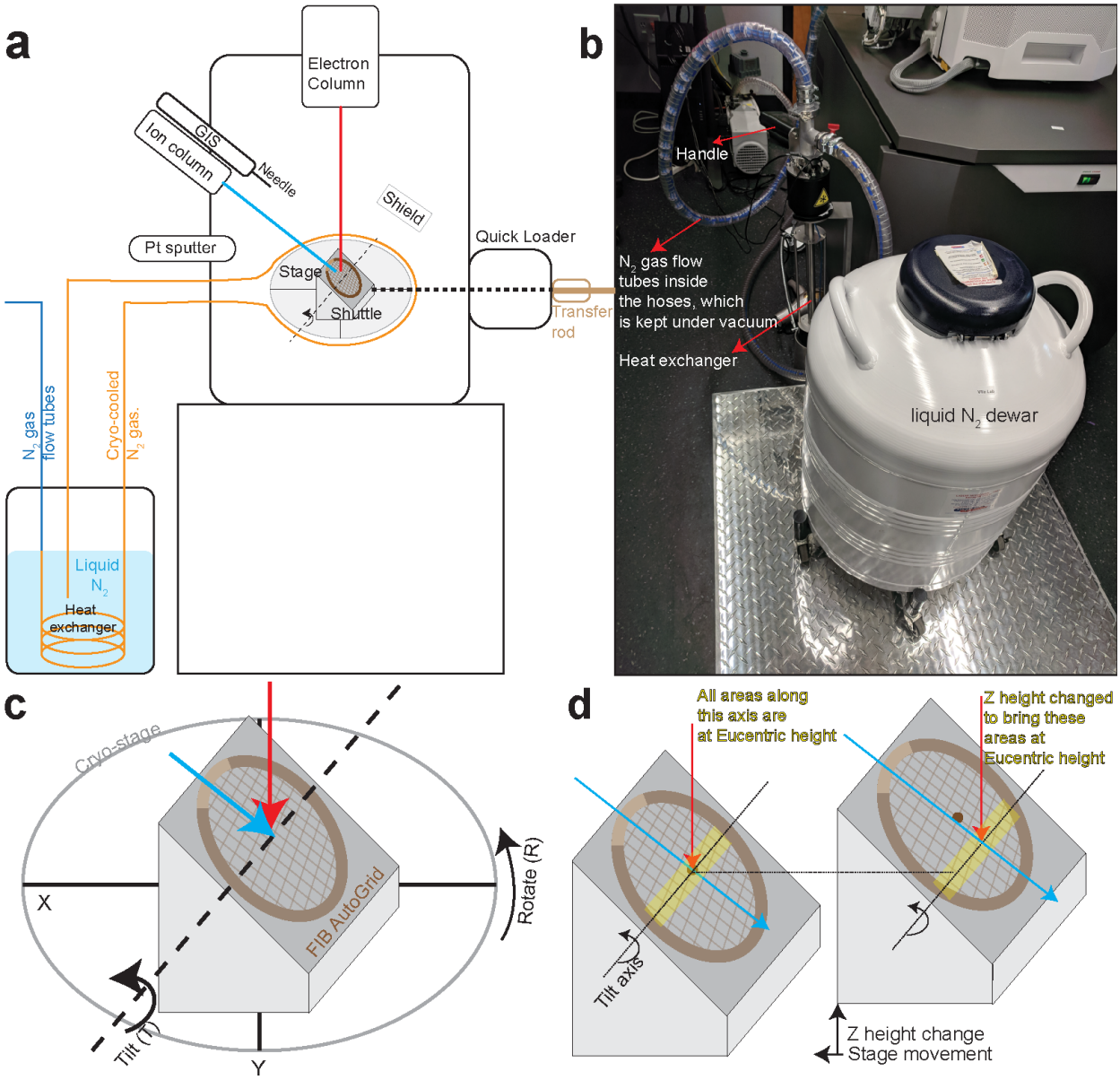

Figure 4| Cryo-stage setup.

a, Schematic of the cryo stage setup inside of cryo-FIB dual beam microscope. The cryo-stage has 5 degrees of freedom which are highlighted in its close-up view. **b,** The heat exchanger with the liquid N_2 dewar. The N_2 flow tubes are enclosed within hoses which are kept under vacuum to provide an insulating environment. **c,** 5 degrees of freedom of the cryo-stage. **d,** The eucentric height is the stage height at which the sample remains centered even when the stage is tilted. For a well-aligned microscope, the electron beam and FIB should be coincident at eucentric height. Therefore, milling should be performed at this height to enable the visualization of the evolving lamella using SEM imaging. Since the grids are held in the shuttle at 45° angles, when moving stage to other areas on EM grids, stage Z height must be changed to bring the areas of interest to be Eucentric height.

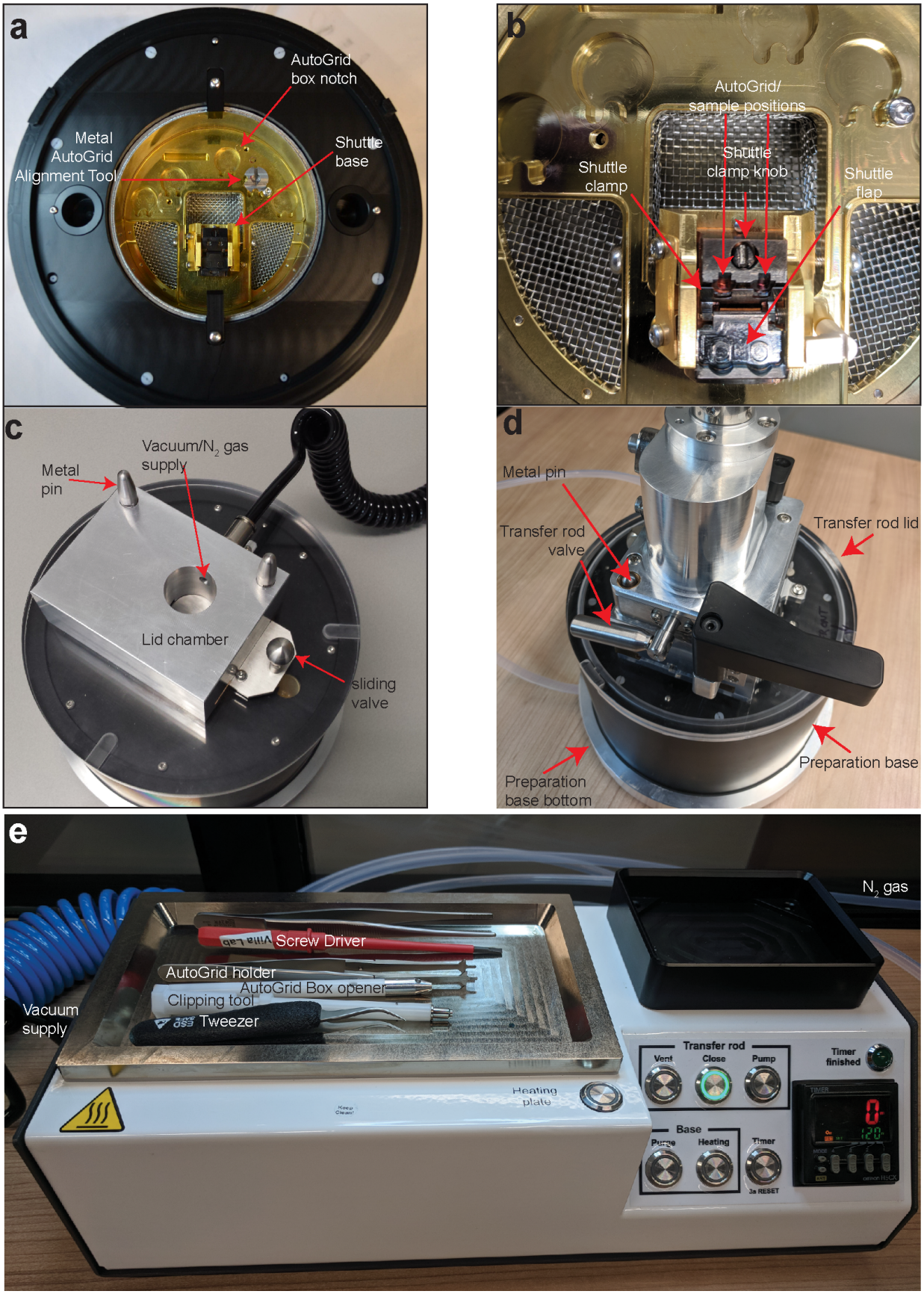
a
AutoGrid
box notch
Metal
AutoGrid
Alignment Tool
Shuttle
base
b
AutoGrid/
sample positions
Shuttle
clamp knob
Shuttle
clamp
Shuttle
flap
c
Vacuum/N2 gas
supply
Metal
pin
Lid chamber
sliding
valve
d
Metal pin
Transfer rod
valve
Transfer rod lid
Preparation
base bottom
Preparation base
e
N2 gas
Screw Driver
AutoGrid holder
AutoGrid Box opener
Clipping tool
Tweezer
Vacuum
supply
Heating
plate
Transfer rod
Vent
Close
Pump
Timer
finished
Base
Purge
Heating
Timer

1

Figure 5| The sample preparation station.
a, The preparation base mounted with metal AutoGrid alignment tool and shuttle at the loading position in the shuttle base. **b**, The shuttle in position for grid loading within the preparation base; shuttle clamp is in the open position. **c,** the preparation base with the lid on; **d**, the transfer rod attached to the preparation base. The preparation base rests on the preparation base bottom that can be used to run N_2 gas through the preparation base, forming a protective gas layer above the liquid N_2 in the base. All images are shown without liquid N_2 for better visibility. **e,** The preparation controller equipped with the heating plate. Various tools used in the protocols are shown.

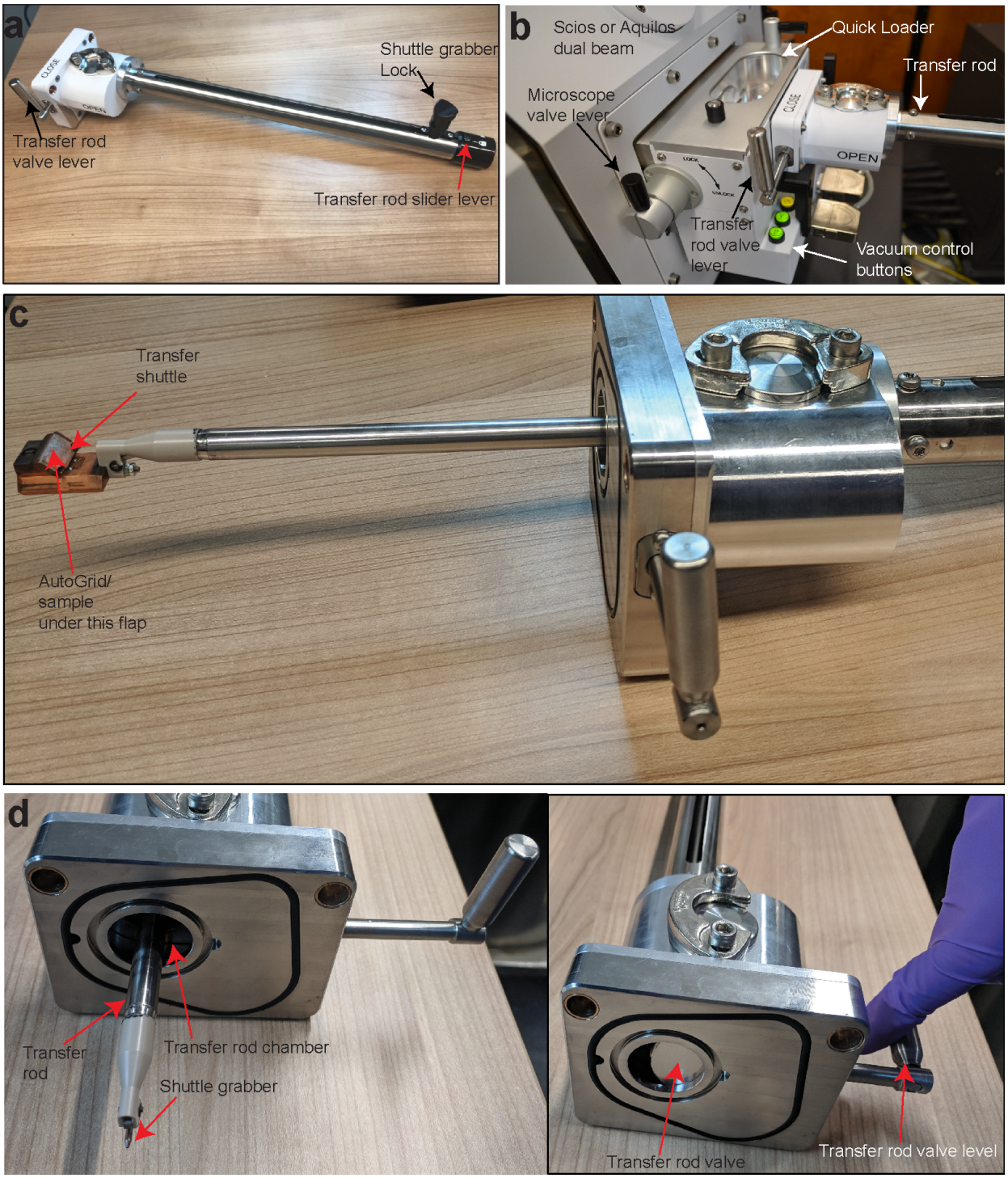

Figure 6| The transfer rod is used for sample transfer under vacuum.
a, The transfer rod position can be fixed from sliding with the transfer rod slider lever. The transfer rod valve lever is used to open/close the transfer rod valve. The shuttle grabber lock controls closes/opens the shuttle grabber to grab/release the shuttle. **b**, Transfer rod attached to the quick loader system. The vacuum control buttons control the quick loader vacuum. **c**, The transfer shuttle is gripped with the transfer rod tip Note: During the shuttle transfer, a flap of the shuttle covers the

grids to minimize the ice contamination under low vacuum condition. **d**, The detail view of the transfer rod.

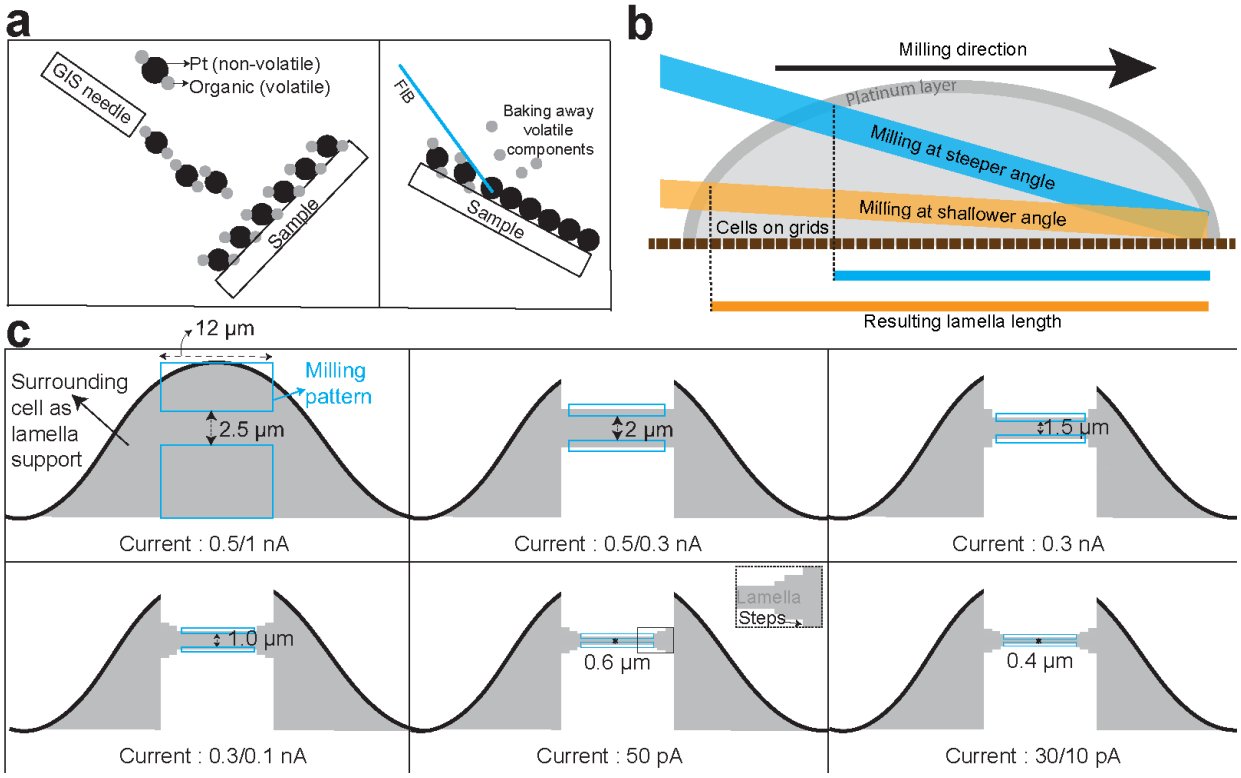

Figure 7| Various procedures/considerations for milling.
a, GIS deposition of organo-platinum followed by the FIB induced baking away of volatile organic components. **b,** Milling angles and resulting lamella lengths along with a layer of GIS-deposition on the front end of the lamella. The milling angle significantly influence the length of the lamellae produced. Milling at shallower angle is particularly important for thin biological samples such as bacterial monolayer. **c**, A schematic representation of the evolution of milling patterns, distances between them and the FIB currents used. Two rectangular milling patterns are selected and positioned to define the area to be sputtered away. These parameters are empirical and vary significantly between different samples.

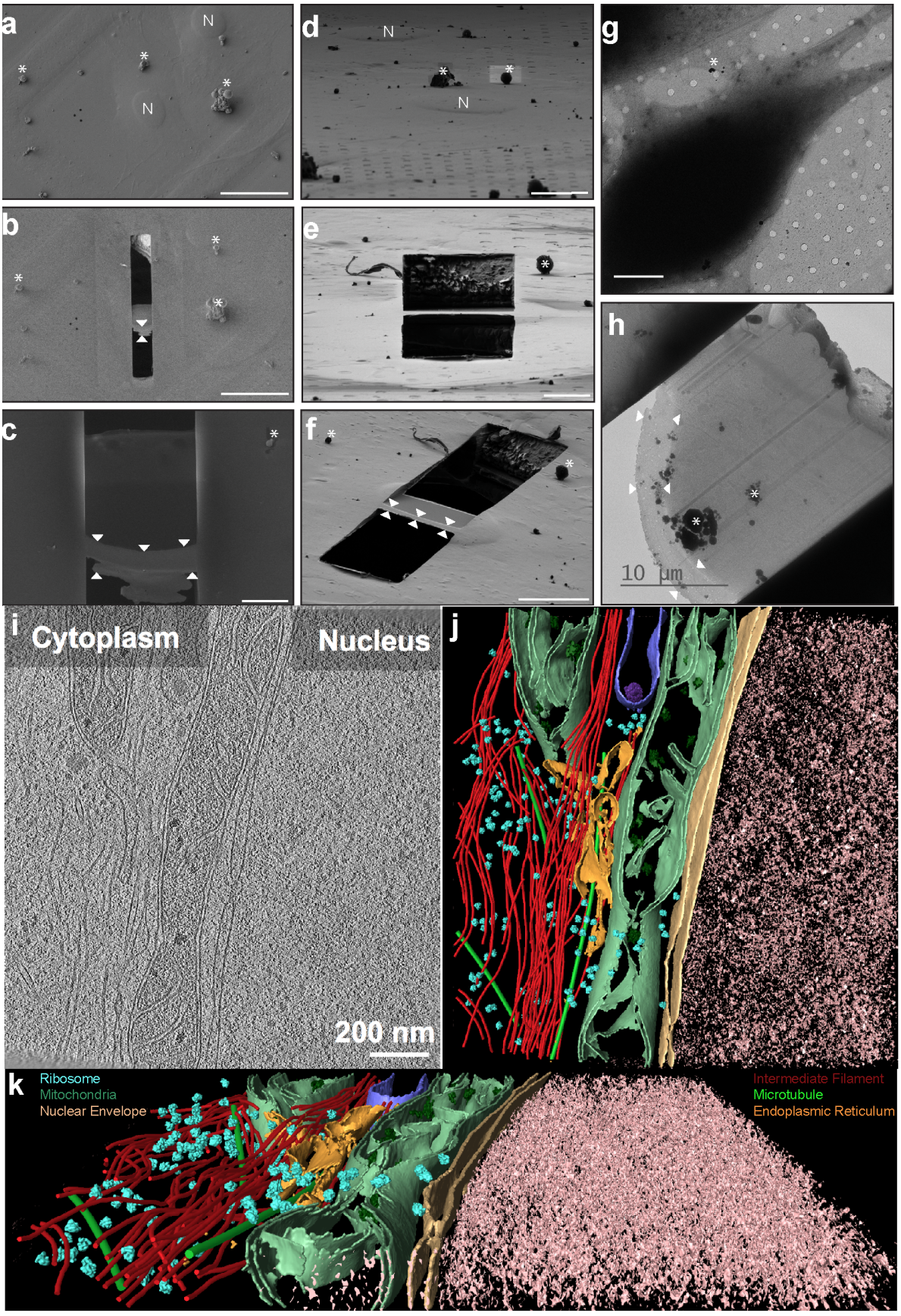
a
N
N
d
N
N
g
b
e
h
10 μm
c
f
i
Cytoplasm
Nucleus
200 nm
j
k
Ribosome
Mitochondria
Nuclear Envelope
Intermediate Filament
Microtubule
Endoplasmic Reticulum

1

Figure 8| A representative data of the cellular cryo-ET using protocol described here. Left panel **(a-c**): SEM images (top view) of vitrified cells. The cell in the center is shown before a, and after b, cryo-FIB milling; image **c,** presents a zoomed in image of b. Middle panel (**d-f**): Images of the same cell taken with the FIB. The cell is shown before (**d**) and after (**e**) cryo-FIB milling; a 45° rotation of the cell is displayed in the image (**f**). Right panel (**g,h**): TEM images of vitrified mammalian cells before (**g**) and after (**h**) milling. The image in **g** illustrates the very limited areas accessible to tomography due to the cell's thickness. Some level of ice contamination (white asterisks) on the sample and even on the lamella is expected and acceptable. The deposited platinum layer is distinguishable from the vitrified sample on the front edge of the milled lamellae (**b, c, f, h**). It is indicated by the white arrowheads. N: nucleus. **i**, The example tomogram taken from milled vitrified mammalian cells (lamella thickness: 150 nm). **j, k**, The corresponding segmented data showing various cellular organelles and cytoskeletons. The subtomogram average of ribosomes from the tomogram is replaced in the segmented data. Annotations of the organellae are shown below. Scale bars (**a**) 40 µm, (**b**) 40 µm, (**c**) 5 µm, (**d**) 10 µm, (**e**) 5 µm, (**f-h**) 10 µm, (**i**) 200 nm.

Figure 9

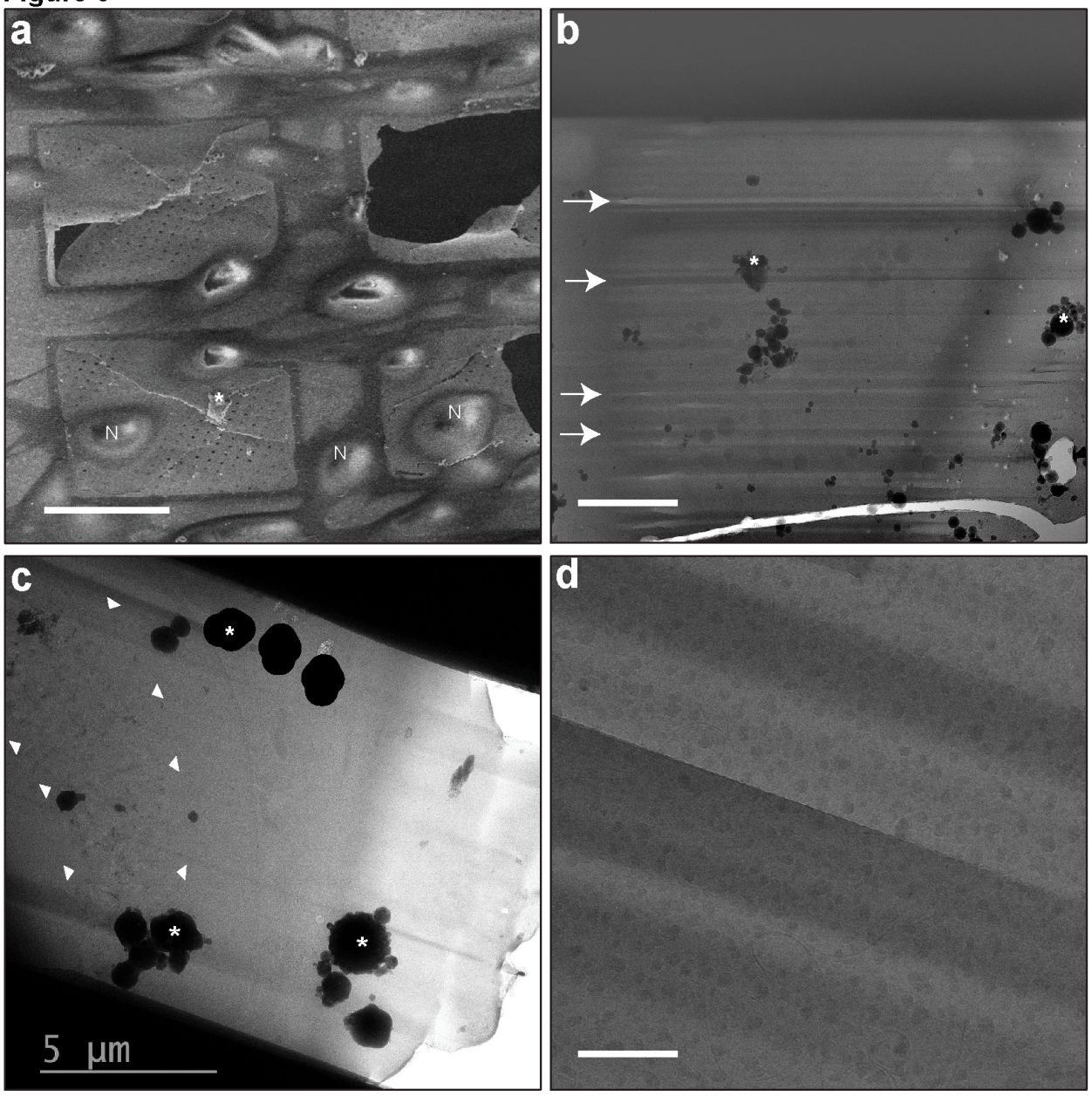

Figure 9| Issues occurring during cryo-FIB milling that require optimization of the workflow **a**, A region of an EM grid with attached NIH/3T3 cells imaged by the SEM. The holey carbon support layer displays holes and cracks. N: nuclei (only 3 are indicated) **b**, A TEM image of a broken lamella (lower part) showing curtains from imperfect milling of the sample (only 4 are indicated by white arrows). **c**, A TEM image of a lamella made from a cell that was not vitrified throughout. White arrowheads indicate the area of crystalline ice in the lamella. A comparison can be made between with a good lamella shown in Fig. 8h. **d**, A high magnification TEM image of a lamella with "leopard ice" contamination. This contamination is due to the compromised stage/shuttle temperature during milling. Dark diagonal stripes arise from curtains of various thicknesses. White asterisks: ice contamination (**b,c**), Scale bars: **a**; 50 µm, **b**; 2 µm, **c**; 5 µm, **d**; 400 nm.

Reference

1. Frank, J. *Three-Dimensional Electron Microscopy of Macromolecular Assemblies: Visualization of Biological Molecules in Their Native State*. *Three-Dimensional Electron Microscopy of Macromolecular Assemblies: Visualization of Biological Molecules in Their Native State* (2010). doi:10.1093/acprof:oso/9780195182187.001.0001
2. Nogales, E. & Scheres, S. H. W. Cryo-EM: A Unique Tool for the Visualization of Macromolecular Complexity. *Mol. Cell* **58**, 677–689 (2015).
3. Erickson, K. D. *et al.* Virion Assembly Factories in the Nucleus of Polyomavirus-Infected Cells. *PLoS Pathog.* **8**, e1002630 (2012).
4. Frank, J. *Electron Tomography: Methods for Three-Dimensional Visualization of Structures in the Cell*. *Vasa* (2006). doi:10.1002/1521-3773(20010316)40:6<9823::AID-ANIE9823>3.3.CO;2-C
5. Grimm, R., Typke, D., Bärmann, M. & Baumeister, W. Determination of the inelastic mean free path in ice by examination of tilted vesicles and automated most probable loss imaging. *Ultramicroscopy* **63**, 169–179 (1996).
6. Pilhofer, M., Ladinsky, M. S., McDowall, A. W., Petroni, G. & Jensen, G. J. Microtubules in Bacteria: Ancient Tubulins Build a Five-Protofilament Homolog of the Eukaryotic Cytoskeleton. *PLoS Biol.* **9**, e1001213 (2011).
7. Beeby, M., Cho, M., Stubbe, J. & Jensen, G. J. Growth and Localization of Polyhydroxybutyrate Granules in Ralstonia eutropha. *J. Bacteriol.* **194**, 1092–1099 (2011).
8. Amat, F. *et al.* Analysis of the Intact Surface Layer of Caulobacter crescentus by Cryo-Electron Tomography. *J. Bacteriol.* **192**, 5855–5865 (2010).
9. Szwedziak, P., Wang, Q., Bharat, T. A. M., Tsim, M. & Löwe, J. Architecture of the ring formed by the tubulin homologue FtsZ in bacterial cell division. *Elife* **3**, (2014).
10. Szwedziak, P., Wang, Q., Freund, S. M. V & Löwe, J. FtsA forms actin-like protofilaments. *EMBO J.* **31**, 2249–2260 (2012).
11. Brandt, F., Carlson, L.-A., Hartl, F. U., Baumeister, W. & Grünewald, K. The Three-Dimensional Organization of Polyribosomes in Intact Human Cells. *Mol. Cell* **39**, 560–569 (2010).
12. Hanein, D. & Horwitz, A. R. The structure of cell–matrix adhesions: the new frontier. *Curr. Opin. Cell Biol.* **24**, 134–140 (2012).
13. Jasnin, M. *et al.* Three-dimensional architecture of actin filaments in Listeria monocytogenes comet tails. *Proc. Natl. Acad. Sci.* **110**, 20521–20526 (2013).
14. Asano, S. *et al.* Proteasomes. A molecular census of 26S proteasomes in intact neurons. *Science* **347**, 439–42 (2015).
15. Beck, M., Lučić, V., Förster, F., Baumeister, W. & Medalia, O. Snapshots of nuclear pore complexes in action captured by cryo-electron tomography. *Nature* **449**, 611–615 (2007).
16. Strauss, M., Hofhaus, G., Schröder, R. R. & Kühlbrandt, W. Dimer ribbons of ATP synthase shape the inner mitochondrial membrane. *EMBO J.* **27**, 1154–1160 (2008).
17. Davies, K. M. *et al.* Macromolecular organization of ATP synthase and complex I in whole mitochondria. *Proc. Natl. Acad. Sci.* **108**, 14121–14126 (2011).
18. Bharat, T. A. M. *et al.* Structure of the immature retroviral capsid at 8A resolution by cryo- electron microscopy . (2012). doi:10.2210/pdb4arg/pdb
19. Li, S., Fernandez, J.-J., Marshall, W. F. & Agard, D. A. Three-dimensional structure of basal body triplet revealed by electron cryo-tomography. *EMBO J.* **31**, 552–562 (2011).

20. Bui, K. H. *et al.* Integrated Structural Analysis of the Human Nuclear Pore Complex Scaffold. *Cell* **155**, 1233–1243 (2013).
21. Briggs, J. A. G. Determination of protein structure at 8.5A resolution using cryo-electron tomography and sub-tomogram averaging. Schur, F. K., Hagen, W. J. H., de Marco, A., Briggs, J. A. G. [J. Struct. Biol. 184 (2013) 394–400]. *J. Struct. Biol.* **198**, 3–4 (2017).
22. Pfeffer, S. *et al.* Structure of the mammalian oligosaccharyl-transferase complex in the native ER protein translocon. *Nat. Commun.* **5**, (2014).
23. Zuber, B. *et al.* Direct Visualization of the Outer Membrane of Mycobacteria and Corynebacteria in Their Native State. *J. Bacteriol.* **190**, 5672–5680 (2008).
24. Salje, J., Zuber, B. & Lowe, J. Electron Cryomicroscopy of E. coli Reveals Filament Bundles Involved in Plasmid DNA Segregation. *Science (80-.).* **323**, 509–512 (2009).
25. Studer, D., Klein, A., Iacovache, I., Gnaegi, H. & Zuber, B. A new tool based on two micromanipulators facilitates the handling of ultrathin cryosection ribbons. *J. Struct. Biol.* **185**, 125–128 (2014).
26. Schur, F. K. M. *et al.* Structure of the immature HIV-1 capsid in intact virus particles at 8.8 Å resolution. *Nature* **517**, 505–508 (2014).
27. Briggs, J. A. G. Structural biology in situ—the potential of subtomogram averaging. *Curr. Opin. Struct. Biol.* **23**, 261–267 (2013).
28. Marko, M., Hsieh, C., Schalek, R., Frank, J. & Mannella, C. Focused-ion-beam thinning of frozen-hydrated biological specimens for cryo-electron microscopy. *Nat. Methods* **4**, 215–217 (2007).
29. Rigort, A. *et al.* Micromachining tools and correlative approaches for cellular cryo-electron tomography. *J. Struct. Biol.* **172**, 169–179 (2010).
30. Hayles, M. F. *et al.* The making of frozen-hydrated, vitreous lamellas from cells for cryo-electron microscopy. *J. Struct. Biol.* **172**, 180–190 (2010).
31. Rigort, A. *et al.* Focused ion beam micromachining of eukaryotic cells for cryoelectron tomography. *Proc. Natl. Acad. Sci.* **109**, 4449–4454 (2012).
32. Wang, K., Strunk, K., Zhao, G., Gray, J. L. & Zhang, P. 3D structure determination of native mammalian cells using cryo-FIB and cryo-electron tomography. *J. Struct. Biol.* **180**, 318–326 (2012).
33. Hsieh, C., Schmelzer, T., Kishchenko, G., Wagenknecht, T. & Marko, M. Practical workflow for cryo focused-ion-beam milling of tissues and cells for cryo-TEM tomography. *J. Struct. Biol.* **185**, 32–41 (2014).
34. Harapin, J. *et al.* Structural analysis of multicellular organisms with cryo-electron tomography. *Nat. Methods* **12**, 634–636 (2015).
35. Zhang, J., Ji, G., Huang, X., Xu, W. & Sun, F. An improved cryo-FIB method for fabrication of frozen hydrated lamella. *J. Struct. Biol.* **194**, 218–223 (2016).
36. Schaffer, M. *et al.* A cryo-FIB lift-out technique enables molecular-resolution cryo-ET within native Caenorhabditis elegans tissue. *Nat. Methods* **16**, 757–762 (2019).
37. Martynowycz, M. W., Zhao, W., Hattne, J., Jensen, G. J. & Gonen, T. Collection of Continuous Rotation MicroED Data from Ion Beam-Milled Crystals of Any Size. *Structure* **27**, 545-548.e2 (2019).
38. Rubino, S. *et al.* A site-specific focused-ion-beam lift-out method for cryo Transmission Electron Microscopy. *J. Struct. Biol.* **180**, 572–576 (2012).
39. Wagenknecht, T., Hsieh, C. & Marko, M. Skeletal muscle triad junction ultrastructure by Focused-Ion-Beam milling of muscle and Cryo-Electron Tomography. *Eur. J. Transl.*

Myol. **25**, 49 (2015).
40. Mahamid, J. *et al.* A focused ion beam milling and lift-out approach for site-specific preparation of frozen-hydrated lamellas from multicellular organisms. *J. Struct. Biol.* **192**, 262–269 (2015).
41. Khanna, K. *et al.* The molecular architecture of engulfment during Bacillus subtilis sporulation. *Elife* **8**, (2019).
42. Chaikeeratisak, V. *et al.* Viral Capsid Trafficking along Treadmilling Tubulin Filaments in Bacteria. *Cell* **177**, 1771-1780.e12 (2019).
43. Engel, B. D. *et al.* Correction: Native architecture of the Chlamydomonas chloroplast revealed by in situ cryo-electron tomography. *Elife* **4**, (2015).
44. Mahamid, J. *et al.* Visualizing the molecular sociology at the HeLa cell nuclear periphery. *Science (80-.).* **351**, 969–972 (2016).
45. Chaikeeratisak, V. *et al.* Assembly of a nucleus-like structure during viral replication in bacteria. *Science (80-.).* **355**, 194–197 (2017).
46. Lopez-Garrido, J. *et al.* Chromosome Translocation Inflates Bacillus Forespores and Impacts Cellular Morphology. *Cell* **172**, 758-770.e14 (2018).
47. Hampton, C. M. *et al.* Correlated fluorescence microscopy and cryo-electron tomography of virus-infected or transfected mammalian cells. *Nat. Protoc.* **12**, 150–167 (2017).
48. Arnold, J. *et al.* Site-Specific Cryo-focused Ion Beam Sample Preparation Guided by 3D Correlative Microscopy. *Biophys. J.* **110**, 860–869 (2016).
49. Watanabe, R. *et al.* The in situ structure of Parkinson's disease-linked LRRK2. *bioRxiv* (2019).
50. Hagen, C. *et al.* Structural Basis of Vesicle Formation at the Inner Nuclear Membrane. *Cell* **163**, 1692–1701 (2015).
51. Buckley, G. *et al.* Automated cryo-lamella preparation for high-throughput in-situ structural biology. *bioRxiv* (2019). doi:https://doi.org/10.1101/797506
52. Zachs, T. *et al.* Fully automated, sequential focused ion beam milling for cryo-electron tomography. *bioRxiv* (2019).
53. Nannenga, B. L. & Gonen, T. MicroED: a versatile cryoEM method for structure determination. *Emerg. Top. life Sci.* **2**, 1–8 (2018).
54. Volkert, C. A. & Minor, A. M. Focused Ion Beam Microscopy and Micromachining. *MRS Bull.* **32**, 389–399 (2007).
55. Ladinsky, M. S. Micromanipulator-assisted vitreous cryosectioning and sample preparation by high-pressure freezing. in *Methods in Enzymology* (2010). doi:10.1016/S0076-6879(10)81008-0
56. Ladinsky, M. S., Pierson, J. M. & McIntosh, J. R. Vitreous cryo-sectioning of cells facilitated by a micromanipulator. *J. Microsc.* **224**, 129–34 (2006).
57. Al-Amoudi, A., Norlen, L. P. O. & Dubochet, J. Cryo-electron microscopy of vitreous sections of native biological cells and tissues. *J. Struct. Biol.* **148**, 131–135 (2004).
58. Al-Amoudi, A. *et al.* Cryo-electron microscopy of vitreous sections. *EMBO J.* **23**, 3583–3588 (2004).
59. Hsieh, C. E., Leith, A. D., Mannella, C. A., Frank, J. & Marko, M. Towards high-resolution three-dimensional imaging of native mammalian tissue: Electron tomography of frozen-hydrated rat liver sections. *J. Struct. Biol.* **153**, 1–13 (2006).
60. Bouchet-Marquis, C., Dubochet, J. & Fakan, S. Cryoelectron microscopy of vitrified sections: a new challenge for the analysis of functional nuclear architecture. *Histochem.*

Cell Biol. **125**, 43–51 (2006).
61. Matias, V. R. F., Al-Amoudi, A., Dubochet, J. & Beveridge, T. J. Cryo-transmission electron microscopy of frozen-hydrated sections of Escherichia coli and Pseudomonas aeruginosa. *J. Bacteriol.* **185**, 6112–6118 (2003).
62. McEwen, B. F., Marko, M., Hsieh, C.-E. & Mannella, C. Use of frozen-hydrated axonemes to assess imaging parameters and resolution limits in cryoelectron tomography. *J. Struct. Biol.* **138**, 47–57
63. Pierson, J. *et al.* Improving the technique of vitreous cryo-sectioning for cryo-electron tomography: Electrostatic charging for section attachment and implementation of an anti-contamination glove box. *J. Struct. Biol.* **169**, 219–225 (2010).
64. Larabell, C. A. & Le Gros, M. A. X-ray Tomography Generates 3-D Reconstructions of the Yeast, Saccharomyces cerevisiae, at 60-nm Resolution. *Mol. Biol. Cell* **15**, 957–962 (2004).
65. Schneider, G. *et al.* Three-dimensional cellular ultrastructure resolved by X-ray microscopy. *Nat. Methods* **7**, 985–987 (2010).
66. Hagen, C. *et al.* Correlative VIS-fluorescence and soft X-ray cryo-microscopy/tomography of adherent cells. *J. Struct. Biol.* **177**, 193–201 (2012).
67. Hagen, C. *et al.* Multimodal nanoparticles as alignment and correlation markers in fluorescence/soft X-ray cryo-microscopy/tomography of nucleoplasmic reticulum and apoptosis in mammalian cells. *Ultramicroscopy* **146**, 46–54 (2014).
68. Wolf, S. G., Houben, L. & Elbaum, M. Cryo-scanning transmission electron tomography of vitrified cells. *Nat. Methods* **11**, 423–428 (2014).
69. Wolf, S. G., Houben, L. & Elbaum, M. Cryo-Tomography of Vitrified Bacterial and Human Cells by Scanning Transmission Electron Microscopy. *Biophys. J.* **106**, 598a (2014).
70. Schertel, A. *et al.* Cryo FIB-SEM: Volume imaging of cellular ultrastructure in native frozen specimens. *J. Struct. Biol.* **184**, 355–360 (2013).
71. Soto, G. E. *et al.* Serial Section Electron Tomography: A Method for Three-Dimensional Reconstruction of Large Structures. *Neuroimage* **1**, 230–243 (1994).
72. Heymann, J. A. W. *et al.* Site-specific 3D imaging of cells and tissues with a dual beam microscope. *J. Struct. Biol.* **155**, 63–73 (2006).
73. Narayan, K. & Subramaniam, S. Focused ion beams in biology. *Nat. Methods* **12**, 1021–1031 (2015).
74. Denk, W. & Horstmann, H. Serial Block-Face Scanning Electron Microscopy to Reconstruct Three-Dimensional Tissue Nanostructure. *PLoS Biol.* **2**, e329 (2004).
75. Helmstaedter, M. *et al.* Connectomic reconstruction of the inner plexiform layer in the mouse retina. *Nature* **500**, 168–174 (2013).
76. Lam, S. S. *et al.* Directed evolution of APEX2 for electron microscopy and proximity labeling. *Nat. Methods* **12**, 51–54 (2015).
77. Shu, X. *et al.* A genetically encoded tag for correlated light and electron microscopy of intact cells, tissues, and organisms. *PLoS Biol.* **9**, e1001041 (2011).
78. Martell, J. D. *et al.* Engineered ascorbate peroxidase as a genetically encoded reporter for electron microscopy. *Nat. Biotechnol.* **30**, 1143–1148 (2012).
79. Ou, H. D. *et al.* ChromEMT: Visualizing 3D chromatin structure and compaction in interphase and mitotic cells. *Science* **357**, (2017).
80. Sochacki, K. A., Shtengel, G., van Engelenburg, S. B., Hess, H. F. & Taraska, J. W.

Correlative super-resolution fluorescence and metal-replica transmission electron microscopy. *Nat. Methods* **11**, 305–308 (2014).
81. Dubochet, J. *et al.* Cryo-electron microscopy of vitrified specimens. *Q. Rev. Biophys.* **21**, 129–228 (1988).
82. de Winter, D. A. M. *et al.* In-situ integrity control of frozen-hydrated, vitreous lamellas prepared by the cryo-focused ion beam-scanning electron microscope. *J. Struct. Biol.* **183**, 11–18 (2013).
83. Schaffer, M. *et al.* Optimized cryo-focused ion beam sample preparation aimed at in situ structural studies of membrane proteins. *J. Struct. Biol.* **197**, 73–82 (2017).
84. Wolff, G. *et al.* Mind the gap: Micro-expansion joints drastically decrease the bending of FIB-milled cryo-lamellae. *J. Struct. Biol.* (2019). doi:10.1016/j.jsb.2019.09.006
85. Mastronarde, D. N. Automated electron microscope tomography using robust prediction of specimen movements. *J. Struct. Biol.* **152**, 36–51 (2005).
86. Mastronarde, D. N. SerialEM: A Program for Automated Tilt Series Acquisition on Tecnai Microscopes Using Prediction of Specimen Position. *Microsc. Microanal.* **9**, 1182–1183 (2003).
87. Hagen, W. J. H., Wan, W. & Briggs, J. A. G. Implementation of a cryo-electron tomography tilt-scheme optimized for high resolution subtomogram averaging. *J. Struct. Biol.* **197**, 191–198 (2017).
88. Kremer, J. R., Mastronarde, D. N. & McIntosh, J. R. Computer Visualization of Three-Dimensional Image Data Using IMOD. *J. Struct. Biol.* **116**, 71–76 (1996).
89. Toro-Nahuelpan, M. *et al.* Tailoring cryo-electron microscopy grids by photo-micropatterning for in-cell structural studies. *bioRxiv* 676189 (2019). doi:10.1101/676189